Factoring the mapping problem: Mobile robot map-building in the Hybrid Spatial Semantic Hierarchy*

Patrick Beeson, Joseph Modayil, and Benjamin Kuipers

The University of Texas at Austin
Department of Computer Sciences

October 2008
Technical Report UT-AI-TR-08-6

Abstract

We propose a factored approach to mobile robot map-building that handles qualitatively different types of uncertainty by combining the strengths of topological and metrical approaches. Our framework is based on a computational model of the human cognitive map; thus it allows robust navigation and communication within several different spatial ontologies. This paper focuses exclusively on the issue of map-building using the framework.

Our approach factors the mapping problem into natural sub-goals: building a metrical representation for local small-scale spaces; finding a topological map that represents the qualitative structure of large-scale space; and (when necessary) constructing a metrical representation for large-scale space using the skeleton provided by the topological map. We describe how to abstract a symbolic description of the robot's immediate surround from local metrical models, how these local symbolic models are combined to build global symbolic models, and how to create a globally consistent metrical map from a topological skeleton by connecting local frames of reference.

1 Introduction

A map is a description of an environment allowing an agent—a human, or in our case a mobile robot—to plan and perform effective actions. From a single location, an agent's sensors can not observe the whole

*This work has taken place in the Intelligent Robotics Lab at the Artificial Intelligence Laboratory, The University of Texas at Austin. Research of the Intelligent Robotics lab is supported in part by grants from the Texas Advanced Research Program (3658-0170-2007), from the National Science Foundation (IIS-0413257, IIS-0713150, and IIS-0750011), and from the National Institutes of Health (EY016089).

structure of a complex, large environment. For this reason, the agent must build a map from observations gathered over time and space. We distinguish between *large-scale space*, with spatial structure larger than the agent's sensory horizon, and *small-scale space*, with structure within the sensory horizon.

Most metrical approaches to mobile robot map-building define a single, global frame of reference in which to create the map. Range measurements are used to perform probabilistic inference about the location of features or about the occupancy of discretized cells in the map [Thrun et al., 2005]. Existing SLAM (simultaneous localization and mapping) methods are highly effective for building local metrical models of small-scale space and for providing reliable localization in the frame of reference of the local map; however, maintaining global consistency over large-scale environments is difficult, particularly when closing large loops in the environment. A popular approach is to use particle filters, where each particle represents a hypothesized exploration trajectory. The researcher must hope that with enough particles the distribution will include one that closes the loop correctly. Since the space of trajectories can be enormous, this hope is often optimistic.

The fundamental problem is representational: loop-closing hypotheses are alternative topological structures for the map, not alternative metrical structures. To be able to solve complex, multi-hypothesis loop-closing problems in a tractable manner, the robot must reason with symbolic topological maps. The space of metrical maps in a single frame of reference does not appropriately represent the states of incomplete knowledge that arise during exploration and map-building in complex, large-scale environments.

Our factored mapping framework is based on the Spatial Semantic Hierarchy (SSH) [Kuipers, 2000, 2008], which uses multiple coordinated representations for knowledge of large-scale space. The *Hybrid SSH* (HSSH) [Kuipers et al., 2004; Beeson, 2008] extends the basic SSH by including representations for small-scale space and defining the relationship between large-scale and small-scale spatial representations. Symbolic topological mapping methods such as the SSH provide a concise representation for the structural alternatives that arise in investigating loop closures. Topological maps provide the ability to store and access multiple local maps with separate frames of reference and topological connections annotated with weak metrical constraints. By separating small-scale from large-scale space, we postpone the problem of coordinating the local frames of reference until the global structure of the topological map has been identified. At that point, the global metrical map can be constructed, efficiently and accurately.

Therefore, our approach factors the mapping problem into four natural sub-goals: (1) building a metrical representation for local small-scale spaces; (2) detecting places and determining their symbolic descriptions; (3) finding a topological map representing the qualitative structure of large-scale space; and (4) constructing a metrical representation for large-scale space in a single global frame of reference, building on the skeleton provided by the topological map. While the global metrical map is useful for some purposes, it is worth noting that many autonomous planning and navigation goals can be achieved effectively using only the global topological map and/or the local metrical maps. Therefore, this approach to hybrid mapping is more

robust than one that extracts topological relations from a global metrical map that must be built first [Thrun and Bücken, 1996].

The multiple representations of the HSSH are described independently, while their semantic dependencies imply that they build on each other. However, this does *not* imply a simple serial processing pipeline. In fact, processing of sensory input to build representations of the different kinds is interleaved, providing various sorts of synergies. Two are particularly important. First, the local metrical map of small-scale space is a useful "observer" both for detecting and describing places and for low-level control with obstacle avoidance. And second, metrical knowledge of relative displacement and then layout of places may be useful for ordering candidate topological maps. Nonetheless, to clarify the distinct representational ontologies, we will describe them in this paper as though they operate independently.

The Hybrid SSH improves mobile robot capabilities in a variety of ways: efficient and robust map-building and navigation, "natural" human-robot interaction due to the multiple representations of space [Beeson et al., 2007], and hierarchical control. This paper cannot cover the full breadth of benefits obtained from using a hybrid topological/metrical framework; thus, this paper focuses solely on the issue of using the Hybrid Spatial Semantic Hierarchy framework for map-building. Here we describe the HSSH theory and demonstrate key points of HSSH map-building using a particular implementation that focuses on perception using range sensors, though other sensory modalities can also be utilized in the HSSH framework—the hybrid, hierarchical framework is largely independent of the sensors used to create the local metrical model of small-scale space (cf. [Murarka et al., 2006]). A more detailed description of the HSSH benefits to control, place detection/description, and human-robot interaction are discussed by Beeson [2008].

2 Background

2.1 Metrical Mapping

Powerful probabilistic methods have been developed for range-sensing mobile robots to perform simultaneous localization and mapping (SLAM) within a single frame of reference [Thrun et al., 2005]. These methods are accurate and reliable for online incremental localization within local neighborhoods. Sensing with sufficiently high frequency relative to local motion guarantees large overlap between successive sensory images. Current sensory information can be compared to the current map in order to improve localization. By analogy with radar signal interpretation, finding the correct match between observations and model is called the *data association* problem. After improved localization occurs, the sensory information is used to update the map for the next SLAM iteration. In local regions, many data association problems, such as the closing of large loops, can be excluded. The absence of large loops means that the problem of large-scale *structural ambiguity* does not arise in the local metrical map.

While metrical SLAM methods work in small spaces, they do not extend well to larger environments.

Global metrical maps become more expensive to update and access without clever storage schemes. More important, is the difficulty that arises when closing large loops (Figure 1). Even with local SLAM methods that use perception to improve the accuracy of localization, odometry error accumulates in the relation between the map's global frame of reference and the ground-truth reference frame of the real-world environment. This global error becomes even more pronounced in environments with long paths that have few distinguishing features. Without proper data association along paths, localization often drifts from the ground-truth, both in the robot's distance along the path and in the robot's heading, causing straight paths to compress, stretch, or curve in the map.

There are ad hoc methods for hypothesizing loop closures when the global odometry error is small. When a large loop is closed, accumulated error will often result in the robot's current observations clashing with older portions of the map. Methods exist that search for a nearby pose in the older portions of the map where perceptions match the prediction (propagating detected global error backwards through the exploration trace) [Lu and Milios, 1997; Hähnel et al., 2003a]; however, these solutions can fail in sufficiently large or complex environments. For example, Cummins and Newman [2008] discuss closing loops over kilometers of travel, where small rotational errors lead to large positional errors, and the correct loop closure may never be considered by odometry-based solutions. Additionally, if the environment is subject to *perceptual aliasing* (different locations look the same), then the matching process may close the loop incorrectly, distorting the map as a whole. Depending on the amount of symmetry in the environment, a single incorrect match can lead the learner down an arbitrarily long "garden path" before the error is discovered. It is still unclear how probabilistic methods applied to metrical maps can properly discover an incorrect map and how they might efficiently backtrack to hypothesize a different loop closure [Hähnel et al., 2003b].

Some research on map-building avoids loop-closing issues by explicitly assuming that the correct data association is known [Leonard and Newman, 2003; Paskin, 2003]. In some cases, even without an explicit assumption about data association, impressive feats of large-scale map-making depend on locations in the environment being sufficiently distinguishable based on local cues [Montemerlo et al., 2002; Konolige, 2004]. Others accept false negative matches in order to avoid false positives, sometimes improperly hypothesizing that a previously seen location is new [Bosse et al., 2003]. This can eliminate the possibility of closing a loop correctly and finding the correct map, which leads to poor planning and navigation performance. In a rich environment with noise due to dynamic changes, it could be that every location is in principle distinguishable, but it is difficult or impossible to know which features identify the place, and which are noise. Methods created to distinguish between perceptually aliased states can get confused under scenarios of *perceptual variability* (the same place looks different on separate occasions) [Kuipers and Beeson, 2002] causing a single physical location to be represented multiple times in the same map.

Early approaches to probabilistic localization and mapping used particles to represent a distribution over robot poses for localization, but a single shared map was updated from the maximum-likelihood pose hy-

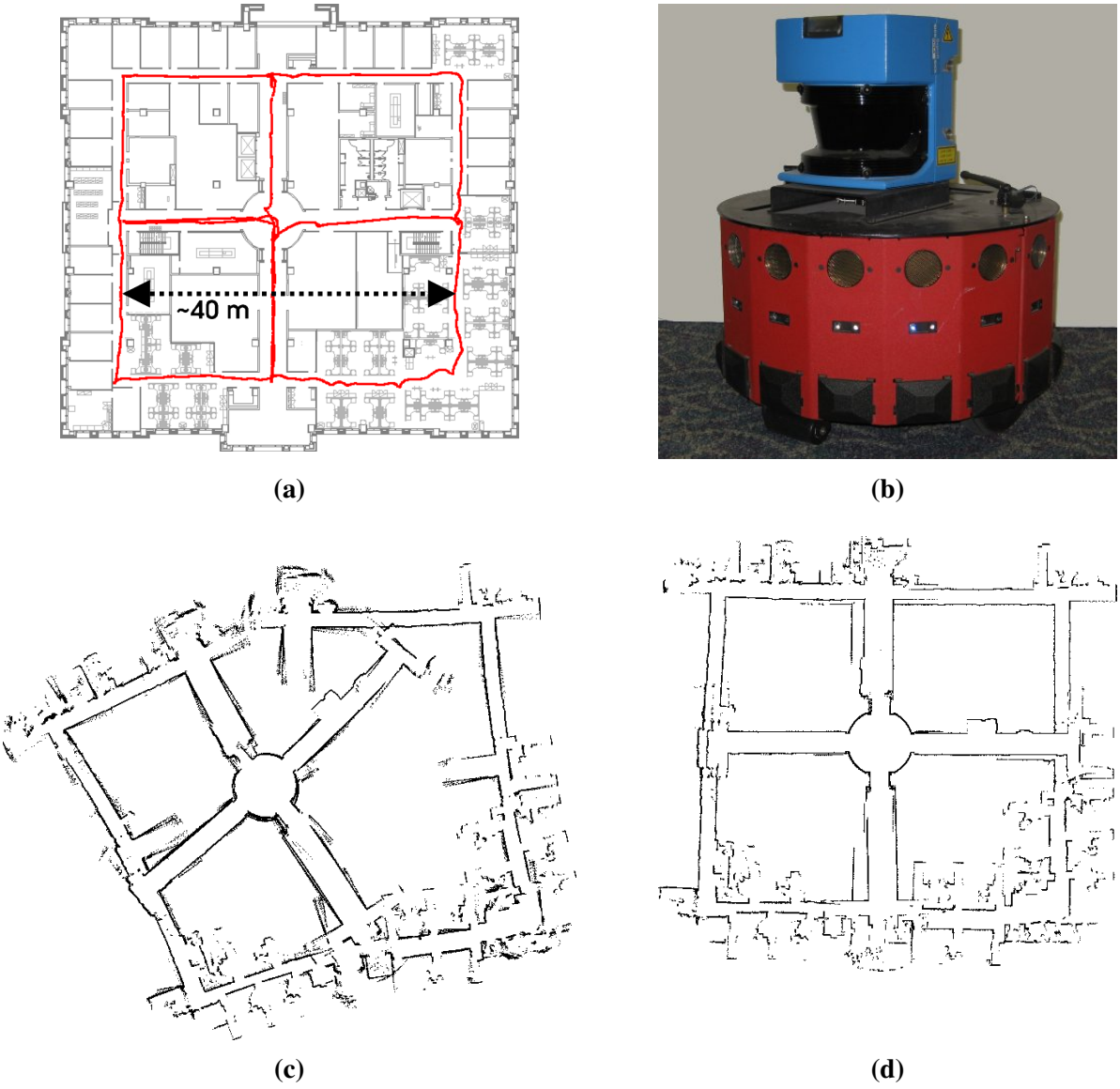

Figure 1: **Closing large loops** reveals problems with cumulative errors when attempting to build metrical maps of large-scale environments in a single global frame of reference. **(a)** This environment and the robot's trajectory through it are used as an example throughout. **(b)** The data comes from a Magellan Pro research robot with differential-drive odometry and a SICK-brand lidar device for precise, planar range-sensing. **(c)** This robot-made map of the environment in image (a) shows the effect of accumulated raw odometry error. **(d)** This map shows the improvement in pose estimation over image (c) by using metrical SLAM methods, but it also shows that significant errors still accumulate with respect to the real environment.

pothesis [Thrun et al., 2000b]. This could produce an incoherent map due to an incorrect and premature commitment to a maximum-likelihood pose hypothesis that turned out to be incorrect. A more principled approach uses Rao-Blackwellized particle filters to explicitly represent the distribution of trajectories and maps by maintaining multiple metrical map hypotheses [Montemerlo et al., 2003; Eliazar and Parr, 2003; Hähnel et al., 2003a]. These methods are run offline (due to computational demands) after exploration is completed, forgoing useful *active exploration* techniques capable of eliminating some loop-closing hypotheses. Additionally, in large, symmetric environments, intractably large numbers of particles may be required to avoid particle depletion when closing large loops. Particle depletion is a failure to have a particle in the distribution that adequately models the correct map.

2.2 Topological Mapping

Topological mapping is the other major paradigm studied in mobile robotics. Cognitive map research supports the creation of topological maps of large, complex environments [Lynch, 1960; Siegel and White, 1975; Kuipers, 1978; Chown et al., 1995; Kuipers, 2000]. A topological map, in its most basic form, represents an environment as a graph where nodes represent places and edges represent connections between places. Several groups of robotics researchers have presented distinct topological implementations that differ in their semantics for the graphs—how they define/describe places and actions between them [Kuipers and Byun, 1991; Mataric, 1992; Shatkay and Kaelbling, 1997; Duckett and Nehmzow, 1999; Choset and Nagatani, 2001; Morris et al., 2005]. Some implementations build topological maps autonomously, some are given topological maps *a priori* [Koenig and Simmons, 1996], and some let the robot explore autonomously while the researcher provides place names to overcome perceptual aliasing issues [Kortenkamp and Weymouth, 1994].

Topological maps are more compact representations than global metrical maps, allowing efficient large-scale planning. Additionally, since the environment is discretized into a graph, movement errors do not accumulate globally. Possibly the most important difference for future robotics research is that topological maps allow compact, efficient hierarchical models that support multi-level symbolic reasoning for robust navigation, planning, and communication.

The major hurdle for topological map-building has been the reliable abstraction of useful symbols from continuous, noisy perceptions of the environment: i.e., how to reliably detect and recognize places and paths. This is an instance of the more general *symbol grounding* problem [Harnad, 1990] that has troubled the AI community for many years. Probabilistic approaches are good at overcoming the kinds of local uncertainty and systematic noise that can hinder reliable symbol extraction. Incorporating probabilistic data association techniques into the topological map-building paradigm has sparked interest in hybrid map-building, including the HSSH approach presented in this paper.

2.3 Hybrid Approaches

Metrical and topological representations for space are very different in character, or more precisely, in ontology. The topological map describes the structure of large-scale space. It abstracts away the specific nature of sensory input and the specific methods used for matching sensory images when the topological map is created. Metrical mapping techniques that rely on local overlap of successive sensations, on the other hand, precisely capture the structure within the local sensory horizon: small-scale space.

Recently, robotics researchers have begun to look at hybrid topological/metrical representations in order to try to leverage the benefits of both approaches. There are too many hybrid approaches to mention here, many with only very subtle differences. We refer the reader to the survey of such approaches by Buschka [2005], as we refer to well-known or prototypical examples in this discussion.

Basically, publications about hybrid metric/topological representations fall into two categories, both of which are addressed by the work in this paper. Many robot implementations use local metrical models as local *observers* that help filter out sensor noise, aggregate observations over time, and create plans that avoid nearby obstacles. There are researchers specifically interested in using metrical models to try to determine qualitatively distinct or interesting places as the robot explores a new environment [Yeap and Jefferies, 1999; Lankenau et al., 2002; Tomatis et al., 2002; Ko et al., 2004]. This is related to our work on grounding places and paths in local metrical models.

The second hybrid approach focuses on using "places" in order to reduce the number of locations in the world that must be considered when hypothesizing metrical loop closures. That is, the goal of most hybrid mapping techniques is still to achieve a global metrical map; however, they use some "topological" (i.e., graph) constraints to make the closing of loops more efficient. Many of these implementations record places arbitrarily [Duckett and Saffiotti, 2000; Zimmer, 2000; Blanco et al., 2008], e.g., every 5 meters traveled, in order to reduce the number of locations in the world where loop closures can occur. Others use a feature buffer, so the robot creates a new place at every n corners or wall segments [Bosse et al., 2003]. Some approaches simply have the researchers press a button to define places in the world [Thrun et al., 1998]. Our research is related to these approaches as well, in that given autonomous place detection at qualitatively distinct and metrically distant places, we can provide a compact graph representation of an environment that makes global metrical mapping extremely efficient.

Finally, a third category of hybrid mapping has only recently been investigated. There has been recent research looking at modeling the full Bayesian distribution over topological hypotheses [Ranganathan et al., 2006; Blanco et al., 2008]. These methods are still strongly grounded in using odometry knowledge (which can be unreliable over large distances [Cummins and Newman, 2007]) and/or aligning raw lidar measurements. As mentioned above, the "places" they utilize are determined by ad hoc means: by the researcher via button presses or by using distance thresholds or finite-sized feature buffers. We believe our compact topological representation is useful here as well. Section 9.2 discusses how this new area of hybrid research

should mesh with the HSSH framework.

The *Hybrid Spatial Semantic Hierarchy (HSSH)* is, to our knowledge, the first framework and implementation to close the loop on the process of going from metrical sensations to both metrical and symbolic models of both small-scale and large-scale space—moving from metrical models of small-scale space to symbolic representations of small-scale space, inferring large-scale structure via symbolic inference, before producing a consistent global metrical model from the symbolic structure. Our approach autonomously detects and describes qualitatively distinct places, creating far fewer places than other "hybrid" approaches. Additionally, these places have meaning as they are inspired by the human cognitive map.

3 The Spatial Semantic Hierarchy

The Spatial Semantic Hierarchy (SSH) [Kuipers, 2000, 2008] represents knowledge of large-scale space with four distinct representations. Figure 2 illustrates the framework. At the SSH Control Level, control laws provide reliable motion among *distinctive states* (dstates) q_i. At the SSH Causal Level, state-action-state *schemas* $\langle q, a, q' \rangle$ explain how the distinctive states are linked by turn and travel *actions*, and relations $o(q) = v$ between a state and its observable *view* describe the potential experiences of the robot. Thus the Causal Level abstracts the continuous world to a deterministic finite automaton [Rivest and Schapire, 1989; Dean et al., 1995], related to the way humans utilize route instructions in navigation. At the SSH Topological Level, a map consisting of places, paths, and regions, describes the connectivity, order, containment, and boundary relations of large-scale environments. At the SSH Metrical Level, local metrical information about the location of obstacles, the magnitudes of actions, the lengths of path segments, and the directions of paths at place neighborhoods are incorporated into local and global metrical maps. One contribution of the Hybrid SSH is to clarify the relation between the metrical information and the symbolic abstractions of the basic SSH levels.

The Spatial Semantic Hierarchy factors spatial uncertainty into distinct components, controlled in distinct ways. *Movement uncertainty* is controlled by the behavior of feedback-driven motion control laws. *Pose uncertainty* is controlled in the basic SSH by hill-climbing to dstates (and in the Hybrid SSH by incremental localization within a local metrical map). *Structural ambiguity* about the large-scale topology of the environment is controlled by search in a space of alternative topological maps. *Global metrical uncertainty* is controlled by relaxing metrical information from separate local frames of reference into a single global frame of reference, guided by the topological map.

3.1 The SSH Control Level

The SSH Control Level describes the system consisting of the agent and its environment as a piecewise continuous dynamical system. The agent's experience is represented at a fine-grained sequence of time-steps

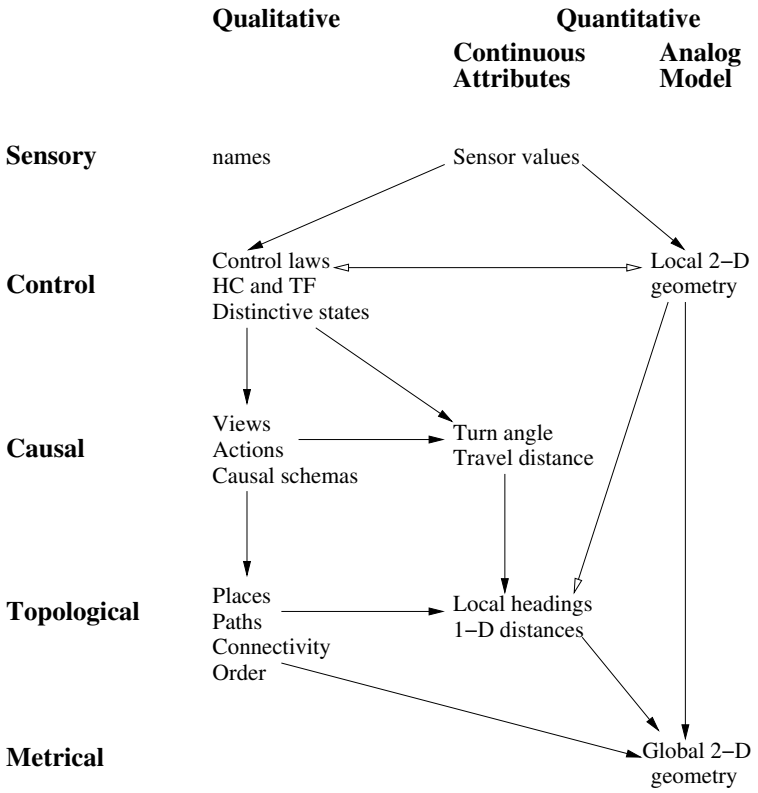

Figure 2: **The Spatial Semantic Hierarchy.** Closed-headed arrows represent dependencies; open-headed arrows represent potential information flow without dependency. (From Kuipers [2000].)

$0 \leq t \leq N$. At any time t, the agent-environment system is described by the state vector x_t (the agent's *pose* in a static world), the agent's sense vector z_t, and its motor vector u_t. We assume that both the environment and the agent's sensory system are very rich, so the sense vector z_t is very high-dimensional.

The dynamical system is described by the following equations, in which the functions F and G represent the physics of the agent's body in the environment and its sensorimotor system respectively. These two functions are not explicitly known or available to the agent. The control law H_i, on the other hand, can be selected by the agent.

$$\begin{aligned} x_{t+1} &= F(x_t, u_t) \\ z_t &= G(x_t) \\ u_t &= H_i(z_t) \end{aligned}$$

The agent acts by selecting a control law H_i to determine its motor output signals as a function of its sensor input. In the basic SSH [Kuipers, 2000], motion is controlled by alternating between two types of controllers. *Trajectory-following* control laws take the robot from one *distinctive state* (dstate) to the neighborhood of another. A *hill-climbing* control law guides the robot to the destination dstate $\bar{x}$ from anywhere in its surrounding neighborhood.

Hill-climbing localizes the agent by moving it reliably to a distinctive state within the local neighborhood, preventing the accumulation of position error, and paving the way for a discrete abstraction of the continuous space. Furthermore, hill-climbing control makes very weak assumptions about the properties of the sensors and the agent's knowledge of those properties; however, hill-climbing control laws can be difficult to define and may vary across domains. An agent often *does* have stronger knowledge of the properties of its sensorimotor system, and physical motion to distinctive states seems awkward and unnecessary in light of that knowledge. A key insight behind the Hybrid SSH is that accurate localization in the small-scale space model of a place neighborhood can substitute for the physical motion of hill-climbing to a particular distinctive state in that neighborhood. In Section 4, we discuss how the Hybrid SSH exploits metrical knowledge of small-scale space to build *local perceptual maps* of place neighborhoods, within which localization is reliable and effective.

3.2 The SSH Causal Level

Given pairs of trajectory-following (TF) and hill-climbing (HC) controls that represent motion between neighboring dstates at the Control Level, we begin to represent the robot's experiences as a set of symbolic abstractions (Figure 3). First, we define an *action* $a \in A$, to represent a pair of trajectory-following and hill-climbing controls that connect dstates. Since the sensory image at a dstate $\bar{z} = G(\bar{x})$ is a point in a very high-dimensional space, it will, in general, never be experienced twice. We will therefore assume

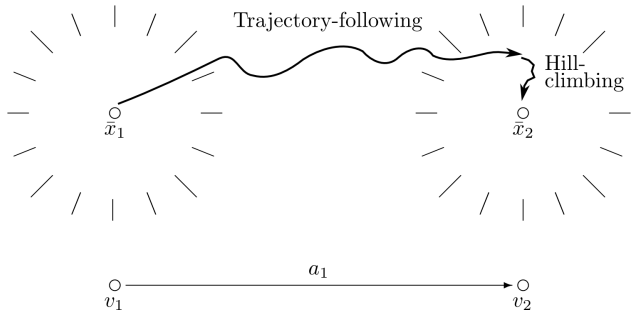

Figure 3: **SSH Control/Causal Level abstraction.** In the SSH, dstates are defined by pairs of trajectory-following and hill-climbing control laws. These sequences are abstracted into actions, and the observations at dstates are abstracted into views. (Adapted from Kuipers [2000].)

that each distinctive state $\bar{x}$ has an associated *view*, $o(\bar{x}) = v \in V$, which is an abstracted description of the sensory image $\bar{z}$. Kuipers and Beeson [2002] describe a bootstrap-learning method for obtaining a view representation suitable for high-performance place recognition. For this paper, we will not require that the observation function o be learned autonomously, but only that it exists.

The SSH Causal Level describes the agent's experience as a deterministic finite automaton (DFA) [Rivest and Schapire, 1989; Dean et al., 1995]. The Causal Level deterministic finite automaton

$$M^C = \langle Q, A, V, R, o \rangle$$

consists of sets of states Q, actions A, observable views V, a transition function $R : Q \times A \rightarrow Q$, and an observation function $o : Q \rightarrow V$. As the robot travels from one distinctive state $\bar{x}$ to the next, its experience is an alternating sequence of views and actions. Some actions are turns, while others are travels.

$$v_0 \quad a_1 \quad v_1 \quad a_2 \quad v_2 \quad \cdots \quad v_{n-1} \quad a_n \quad v_n$$

At the SSH Control Level, a view v_i is experienced only when the agent is at a distinctive state $\bar{x}_i$, so the view v_i is an observable manifestation of the distinctive state: $v_i = o(\bar{x}_i)$.

$$\begin{array}{ccccccccc} \bar{x}_0 & a_1 & \bar{x}_1 & a_2 & \bar{x}_2 & \cdots & \bar{x}_{n-1} & a_n & \bar{x}_n \\ | & & | & & | & & | & & | \\ v_0 & & v_1 & & v_2 & \cdots & v_{n-1} & & v_n \end{array}$$

At the Causal Level, each state $q \in Q$ represents an equivalence class of distinctive states $\bar{x}$ in the physical

world.[1] Two distinctive states $\bar{x}_i$ and $\bar{x}_j$ are equivalent if they represent different experiences of the same distinctive state $q \in Q$. (We use the notation $[\bar{x}_i] = [\bar{x}_j] = q$ for this.) The set Q of distinctive states thus represents a specific hypothesis about which experiences $\bar{x}_i$ represent repeated encounters with the same state q in the environment; that is, Q specifies *data association* for loop closures.

All distinctive states in the same equivalent class q must have the same view.[2]

$$[\bar{x}] = [\bar{x}'] \rightarrow o(\bar{x}) = o(\bar{x}')$$

Thus, $o(q)$ is well-defined, and we can write

$$q = q' \rightarrow o(q) = o(q')$$

The full sensory input from high bandwidth sensors in a realistically complex environment is so rich that sensory images will never match exactly. Views must be defined in terms of some observation function that allows the same dstate to be reliably detected on separate occasions. Thus, an experience with repeated states such as

$$\begin{array}{ccccccccc} q_0 & a_1 & q_1 & a_2 & q_2 & \cdots & q_0 & a_n & q_1 \\ | & & | & & | & & | & & | \\ v_0 & & v_1 & & v_2 & \cdots & v_{n-1} & & v_n \end{array}$$

can only be consistent if $v_{n-1} = v_0$ and $v_n = v_1$. However, abstracted views are subject to perceptual aliasing (different places look the same), leading to ambiguities about the topological structure of the map: $o(q) = o(q') \not\rightarrow q = q'$.

The *transition function* $R : Q \times A \rightarrow Q$ is represented as a set of *schemas* $r = \langle q, a, q' \rangle$, where $context(r) = q$, $action(r) = a$, and $result(r) = q'$. As new observations are added to the robot's experience, new schemas $\langle [\bar{x}_n], a_{n+1}, [\bar{x}_{n+1}] \rangle$ are learned by the transition function R. The causal map is constructed by searching for an appropriate set Q of states (i.e., equivalence classes of distinctive state observations), such that M^C has a deterministic transition function R, predicted and observed views are consistent, and M^C is consistent with the axioms for topological maps [Remolina and Kuipers, 2004].

For the purpose of building the SSH Causal Level from exploration experience, building and using a DFA is far more tractable than building and using a probabilistic state model, such as a hidden Markov

[1] The term *distinctive state*, abbreviated *dstate*, is thus overloaded. It refers both to the state $\bar{x}$ resulting from a hill-climbing control law at the SSH Control Level, and to the state $q = [\bar{x}]$ at the SSH Causal Level which is part of the discrete abstraction of the continuous environment. It is this abstraction from continuous to symbol that facilitates causal/topological mapping in the basic SSH.

[2] The axioms provided here describe the nature of the spatial knowledge represented at each SSH level, but we omit auxiliary axioms required for logical completeness (e.g., unique names axioms, etc). A complete set of axioms is provided by Remolina and Kuipers [2004]. For clarity and conciseness, we use a typed logic in which variable names encode their types, and we assume that all free variables in axioms are universally quantified.

model (HMM).[3] The key benefit of a DFA over HMMs (or stochastic finite automata in general) are that both the transition function and the observation function are deterministic. The deterministic transition function follows from the nature of the abstraction that results from moving reliably between dstates via TF and HC control laws. The deterministic observation function follows from the abstraction that defines the observation function o. One improvement of the HSSH over the SSH is that local small-scale space models make place detection and observational classification of states deterministic without the need for hill-climbing (Section 5).

The effect of the SSH hill-climbing (and HSSH place detection and localization) is that the Causal Level representation can assume that actions are deterministic. The determinism of the observation function rests on the abstraction from sensory images to views being sufficiently aggressive to eliminate perceptual *variability*. Although observations are deterministic, they are not necessarily unique since there may still be perceptual aliasing. This ambiguity is handled by creating multiple hypotheses of topological (thus causal) models, as explained in Section 3.3. In general, it is not possible for a robot to recover the complete spatial structure of any arbitrary environment [Dudek et al., 1991]; therefore, keeping around the tree of possible maps allows the robot to continue navigation when the best hypothesis is refuted by an experienced counter example.[4]

3.3 The SSH Topological Level

In the SSH, a topological map is an instantiated model for two sets of axioms: one that describes topological maps in general and another that describes the exploration experience of the agent in a particular environment. We identify the global topological map by generating potential models of these axioms, discarding those that violate the axioms, and applying an ordering on the remaining ones so that a single best model can be selected. If there is no single best model, then a few closely competing models can be identified and can be used to make an exploration plan to help discriminate between models.

The SSH Topological map M^T describes the environment in terms of dstates, places, paths, regions, and the qualitative relations among them such as connectivity, order, and containment. A dstate $q \in Q$ represents a distinctive state or pose of the agent in the environment, a place $p \in P$ represents a zero-dimensional location, a path $\pi \in \Pi$ represents a one-dimensional structure, and a region $r \in R$ represents a two-dimensional subset of the environment. In this paper, we will not discuss regions or their relations,

[3] Finding the minimal DFA in the general case, like finding the minimal HMM, is NP-Complete [Gold, 1978; Angluin, 1978]. However, given non-symmetries in the environment, it is possible to use active exploration routines to eliminate many DFA hypotheses. Active exploration routines that eliminate ambiguity among DFA hypotheses are closely related to *adaptive distinguishing sequences*, which can be computed in polynomial time [Yannakakis and Lee, 1991], and should allow the robot to find a minimal DFA in polynomial time [Schapire, 1991] in future work on active exploration.

[4] Long-term experience with the HSSH has yielded deterministic actions and views in research settings, but we can envision rare scenarios, e.g., an intersection crowded with people, that could lead to an undetected or misclassified place. Detecting and understanding these unusual events should allow us to still assume deterministic actions $(100-\varepsilon)\%$ of the time.

which are described by Remolina and Kuipers [2004].

We formalize a topological map as

$$M^T = M^C \cup Objects \cup Relations.$$

Here $Objects = \langle P, \Pi, R \rangle$, where P is a set of places, Π is a set of paths, and R is a set of regions. M^T thus includes (via M^C) the sets of states, actions, and views. *Relations* encodes the relations over this set of objects. These relations, including *at*, *along*, *on*, *order* (and the "star" relations that describe the local topology of places), allow for a richer description of the connectivity of places and paths, and are introduced below as needed.

At the SSH Causal Level, the experience is represented as an alternating sequence of states ($q_i \in Q$) and actions ($a_j \in A$).

$$q_0 \quad a_1 \quad q_1 \quad a_2 \quad q_2 \quad \cdots \quad q_{n-1} \quad a_n \quad q_n$$

At the Topological Level, each distinctive state $q \in Q$ corresponds to being *at* a place, and facing *along* a path in some direction. Since a path is one-dimensional, it has two directions $d \in \{+,-\}$, for which $opp(+) = -$ and $opp(-) = +$. We define a directed path, π^d, to represent facing along a path in a particular direction.

$$\forall q \in Q \; \exists p \in P, \; \pi \in \Pi, \; d \in \{+,-\} \; [at(q,p) \; \wedge \; along(q,\pi,d)] \tag{1}$$

$$along(q,\pi^d) \equiv along(q,\pi,d)$$

Additionally, there are two kinds of basic actions, turns and travels, and there is a TurnAround action.

$$A = Turns \cup Travels \qquad TurnAround \in Turns$$

A place $p \in P$ corresponds to a set of states linked by turn actions.

$$\langle q,a,q' \rangle \in S \wedge a \in Turns \wedge at(q,p) \rightarrow at(q',p) \tag{2}$$

Similarly, a path $\pi \in \Pi$ corresponds to a set of states linked by travel actions, or by a TurnAround.

$$\langle q,a,q' \rangle \in S \wedge a \in Travels \wedge along(q,\pi,d) \rightarrow along(q',\pi,d) \tag{3}$$

$$\langle q,a,q' \rangle \in S \wedge a = TurnAround \wedge along(q,\pi,d) \rightarrow along(q',\pi,opp(d)) \tag{4}$$

The relation $on(\pi,p)$ means that the place $p \in P$ is on the path $\pi \in \Pi$.

$$at(q,p) \wedge along(q,\pi,d) \rightarrow on(\pi,p) \tag{5}$$

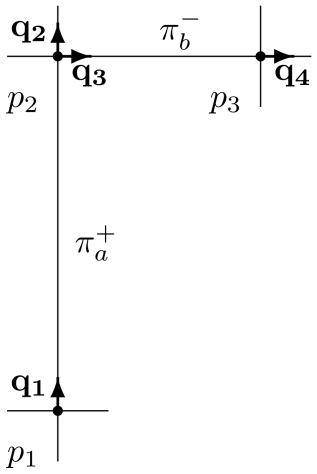

Causal schema	Equation #	Topological relation
$\langle q_1, travel, q_2\rangle \in S$	(1) $\rightarrow$	$at(q_1, p_1)$, $along(q_1, \pi_a^+)$
	(5) $\rightarrow$	$on(\pi_a, p_1)$
	(3) $\rightarrow$	$along(q_1, \pi_a^+)$, $along(q_2, \pi_a^+)$
	(1) $\rightarrow$	$at(q_2, p_2)$
	(5) $\rightarrow$	$on(\pi_a, p_2)$
	(6) $\rightarrow$	$order(\pi_a^+, p_1, p_2)$
	(8) $\rightarrow$	$p_1 \neq p_2$
$\langle q_2, turn, q_3\rangle \in S$	(2) $\rightarrow$	$at(q_3, p_2)$
	(1) $\rightarrow$	$along(q_3, \pi_b^-)$
	(5) $\rightarrow$	$on(\pi_b, p_2)$
$\langle q_3, travel, q_4\rangle \in S$	(3) $\rightarrow$	$along(q_4, \pi_b^-)$
	(1) $\rightarrow$	$at(q_4, p_3)$
	(5) $\rightarrow$	$on(\pi_b, p_3)$
	(6) $\rightarrow$	$order(\pi_b^-, p_2, p_3)$
	(8) $\rightarrow$	$p_2 \neq p_3$

Figure 4: **Topological abduction example.** Here we illustrate the abduction process, using the topological axioms to model exploration. Starting at dstate q_1, the agent reaches dstate q_2 at a place p_2 having traveled along directed path π_a^+. It then turns to dstate q_3, still at place p_2, and is ready to travel along another path, say π_b^-, from q_3 to dstate q_4 at some other place.

A path defines an order relation over the places on it:

$$\langle q, a, q'\rangle \in S \wedge a \in Travels \wedge at(q, p) \wedge at(q', p') \wedge along(q, \pi, d) \rightarrow order(\pi, d, p, p') \tag{6}$$

$$order(\pi, d, a, b) \rightarrow on(\pi, a) \wedge on(\pi, b) \tag{7}$$

$$\neg order(\pi, d, p, p) \tag{8}$$

$$order(\pi, d, a, b) \iff order(\pi, opp(d), b, a) \tag{9}$$

$$order(\pi, d, a, b) \wedge order(\pi, d, b, c) \rightarrow order(\pi, d, a, c) \tag{10}$$

In order to create a Topological Level map from a Causal Level experience, such as $\langle q_1, travel, q_2\rangle$, $\langle q_2, turn, q_3\rangle$, $\langle q_3, travel, q_4\rangle$, the agent uses abduction to hypothesize the existence of several places and paths at which these distinctive states occur. Figure 4 shows an example of the abduction process.

Remolina and Kuipers [2004] provide a non-monotonic axiomatization of the SSH topological map, including additional elements of the theory (regions, boundary relations, and metrical relations), along with more details and motivating examples. This theory provides a precise specification of the possible logi-

cal models (topological maps) that are consistent with the axioms and the sequence of actions and views observed while exploring. A prioritized circumscription policy (expressed as a nested abnormality theory [Lifschitz, 1995]) specifies how distinct consistent logical models are ordered by simplicity. Furthermore, Savelli and Kuipers [2004] have developed the non-local *planarity constraint*, which enforces the requirement that a topological map is a graph embedded in the plane. Figure 5 presents an algorithm for constructing all possible topological maps by generating all possible sets Q.

3.4 The SSH Metrical Level

The SSH, often thought of as a framework for creating purely topological maps, has always allowed for local metrical knowledge to be utilized at the Control Level (Figure 2, right column). Additionally, the SSH Metrical Level has always supported a global metrical map to be created *after* the topological map—it is our belief that such a global metrical map is often unnecessary for navigation in and communication about large-scale environments. However, the SSH theory has lacked a formal description of exactly how metrical information influences the hierarchical abstractions of space. One contribution of this paper is to clarify the relationships between metrical and symbolic knowledge in a navigational agent.

In work leading to the development of the SSH, Kuipers and Byun [1991] created a "patchwork metrical map". Their mapping implementation annotated topological places and paths with metrical data gathered during exploration. Given a topological map hypothesis, the global place layout was relaxed to minimize errors with respect to the annotated metrical data before adding stored range information to create the obstacle map. This approach is similar to the probabilistic techniques we define formally in Section 7.3.

3.5 Extending the SSH

The Spatial Semantic Hierarchy depends on the assumption that the environment naturally decomposes into place neighborhoods, connected by path segments, which can then be abstracted to a topological map. That is, it uses the sparse structure of man-made environments (or man-made paths in natural environments) to define a small number of discrete places and connecting paths. Obviously, topological structure may be imposed even in unstructured environments. Defining places at visually distinctive locations along a single path (e.g., a water tower on the side of a highway) or even based on metrical path-integration in wide-open spaces (as the Puluwat navigators do when piloting dugout canoes between distant islands [Gladwin, 1970]) are currently not handled by our SSH hill-climbing controllers or the HSSH place detection methods. We believe these type of places can be represented within the SSH framework, but we leave this problem for future work.

The basic SSH makes weak (i.e., very general) assumptions about the sensory capabilities of the navigational agent; thus, abstraction from continuous sensations to discrete models of the environment depends

0. Perform initial action a_0 that brings the robot to a place along a directed path. Initialize the tree of maps with the map hypothesis $\langle M_0, q_0 \rangle$, where M_0^C contains the single dstate q_0 with its observed view v_0, and M_0^T contains the single place p_0 and path π_0.

After performing a new action a and observing the resulting view v, for each consistent map $\langle M, q \rangle$ on the fringe of the tree:

1. If M^C includes $\langle q, a, q' \rangle$ in R and $v' = o(q')$,
   - if $match(v, v')$, then $\langle M, q' \rangle$ is the successor to $\langle M, q \rangle$, extending the tree;
   - if not, then mark $\langle M, q \rangle$ as inconsistent.
2. Otherwise, M^C does not include $\langle q, a, q' \rangle$ in R. Let M' be M extended with a new distinctive state symbol q' and the assertions $v = o(q')$ and $\langle q, a, q' \rangle$. Consider the $k \geq 0$ dstates q_j in M with $v_j = o(q_j)$, such that $match(v_j, v)$. Then $\langle M, q \rangle$ has $k+1$ successors:
   - $\langle M'_j, q' \rangle$ for $1 \leq j \leq k$, where M'_j is M' extended with the assertion $q' = q_j$.
   - $\langle M'_{k+1}, q' \rangle$, where M'_{k+1} is M' extended with the k assertions that $q' \neq q_j$, for $1 \leq j \leq k$.
3. Mark a new successor map inconsistent if it violates the axioms of topological maps.
4. Define a preference order on the consistent maps at the leaves of the tree.

In the Basic SSH:

$M = M^T$.
A view is a simple symbol.
$match(v, v')$ iff $v = v'$.
Both $a \in Turns$ and $a \in Travels$ can reach step 2 and cause a branch.
Preference order from prioritized circumscription policy [Remolina and Kuipers, 2004].

In the Hybrid SSH (Section 6):

$M = \langle M^T, M^P \rangle$.
A view is a structure $\langle S_p, \tilde{\pi}^d \rangle$, where $p = place(q)$, consisting of a local topology and the directed local-path the robot arrived upon.
$match(v, v')$ iff there exists an isomorphism $\phi : S_p \rightarrow S'$ where $\phi(q) = q'$.
Only $a \in Travels$ can reach step 2 and cause a branch.
Future work: Preference order from map probabilities (Section 9.2).

Figure 5: **Building the tree of topological maps.** This pseudo-code framework describes the algorithm for building a tree of all possible topological consistent with a sequence of actions and observations at discrete places. The different instantiations of this framework for the basic and hybrid SSH are also described.

on well-crafted control laws that move the robot reliably between distinctive states. The Hybrid SSH makes stronger (i.e., more specific) assumptions about the types of sensors available to the agent, for example, range sensors. This allows the HSSH to extend the basic SSH by using existing metrical mapping techniques to create precise observational models of the local surround.

The HSSH has four major levels of representation that correspond to the four SSH levels (Figure 6). At the *Local Metrical Level*, the agent builds and localizes itself in the Local Perceptual Map (LPM), a metrically accurate map of the local space within its sensory horizon. The LPM is used for local motion planning and hazard avoidance. At the *Local Topological Level*, the agent identifies discrete places (e.g., corridor intersections, rooms, etc.) in the large-scale continuous environment, and qualitatively describes the configuration of the paths through the place—its local decision structure. At the *Global Topological Level*, the agent resolves structural ambiguities and determines how the environment is best described as a graph of places, paths, and regions. The *Global Metrical Level* specifies the layout of places, paths, and obstacles within a single global frame of reference. It can be built on the skeleton provided by the topological map. Figure 6 diagrams the basic flow of data in the HSSH, from sensors, through the local metrical model of small-scale space and the local and global symbolic models of the large-scale environment, finally creating the global metrical model if desired.

Having small-scale space models of the local surround creates several advantages when implementing the HSSH versus the basic SSH. First, the robot represents the local environment using a *local perceptual map (LPM)* (Section 4). The robot can therefore use algorithms for local metrical motion planning and obstacle avoidance instead of relying on behavior-based controllers. Second, metrical localization can be done quickly after entering a place neighborhood, rather than requiring physical hill-climbing to a distinctive pose.

A symbolic description of the *local topology* is extracted from this precise small-scale-space model of the local surround via *gateways* (Section 5). Thus, the view of a distinctive state no longer need be some user-defined function of the perceptual inputs. Instead, the method relies on the local topology extracted from the LPM to describe places, thus describing all distinctive states at each place. Using local topology to *detect and describe* places allows the robot to model more complicated intersections of paths than with hill-climbing. Additionally, using local topology constrains the global topological model search (Section 6), as branching in the tree of possible maps occurs only when arriving at a place, not when visiting the various dstates of a place.

Stored metrical information along topological connections between places can be used to efficiently obtain a global metrical layout of places (Section 7), which provides the "backbone" for a global map if desired. The HSSH also improves navigational behaviors and facilitates multi-modal human-robot interaction [Beeson et al., 2007; MacMahon et al., 2006].

The rest of this paper is focused on discussion of the individual components of the HSSH. Section

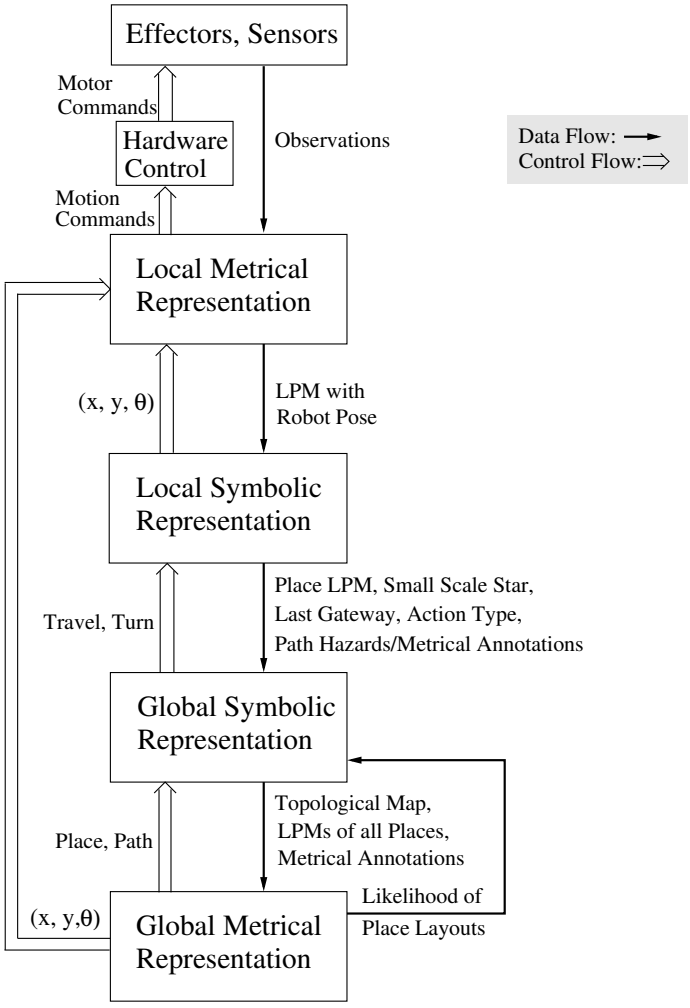

Figure 6: **HSSH description.** The HSSH is an integrated framework of multiple, distinct representations of spatial knowledge. Each level of abstraction uses its own ontology with concepts motivated by human cognitive abilities and grounded to the environment via local metrical observations. The four major components here correspond to the four levels of the basic SSH shown in Figure 2.

4 describes local metrical modeling of small-scale space using existing SLAM methods, as well as local motion planning. Section 5 describes how the local topology of a place is abstracted from the local metrical model and how this abstraction leads to reliable place detections and descriptions. Section 6 describes how the global topological map is created and maintained as exploration provides a sequence of actions and local topologies of places encountered during travel. Section 7 describes how the global metrical map is built on the qualitative skeleton provided by the global topological map. Section 8 summarizes the paper, and Section 9 discusses future research on optimizing the HSSH.

4 HSSH Local Metrical Level

The critical difference between the basic SSH and the Hybrid SSH is the use of a local metrical model of small-scale space surrounding the robot. In our current work, we call this model a local perceptual map (LPM). The LPM is currently built using sensor input from laser range sensors that see walls, but the LPM could be built from visual sidewalk (or road) detection or other sensor modalities. Similarly, the current LPM representation models occupied, free, and unknown regions of space. Work by Murarka et al. [2006] investigates incorporating semantic labels into the LPM to denote drop offs, pedestrians, and other types of hazards.

4.1 Local Perceptual Map (LPM)

The *local perceptual map* (LPM) is a bounded-size metrical description of the small-scale space surrounding the agent. It functions as an *observer*, integrating sensor values over time to determine the locations of obstacles and other hazards, for localization, motion planning, and the derivation of local features for larger-scale mapping. The LPM represents the small-scale space within the robot's sensory horizon, not just what is currently in view. It is small enough to avoid the problem of closing large loops. The frame of reference of the LPM is local. Its relation with the world frame may be unknown, and will drift over time due to accumulating errors.

When the agent travels from one place to another, the LPM acts as a *scrolling map*, $\tilde{m}$, that describes the robot's immediate surround. Information that scrolls off the LPM is discarded, and new cells that scroll onto the map are initialized as unknown.[5] Because the LPM has a fixed, bounded size, the cost of updating it is constant in both time and space.

The full task of building metrical maps from exploration data can be described as finding the joint posterior over maps m and trajectories $x = (\mathsf{x}, \mathsf{y}, \theta)$ in $P(x, m|z, u)$ with the following symbol definitions.

[5] Our rectangular LPM scrolls, horizontally or vertically, as needed to keep to keep the robot's pose in a central cell. Information in the occupancy grid is only shifted by integral numbers of cells to avoid blurring the model by rotations or partial-cell translations.

t	The time-steps $0 \leq t \leq N$ of the agent's experience.
$x = x_{0:N}$	The sequence of agent poses x_t at each time-step t.
$z = z_{0:N}$	The sequence of observations z_t.
$u = u_{1:N}$	The sequence of actions u_t between time-steps.
m	The set of map elements, which may be landmarks or occupancy grid cells. $\tilde{m}$ (the scrolling local perceptual map) is a particular example of a metrical map m.

The joint probability of the pose history x and the metrical map m can be decomposed as

$$P(x,m|z,u) = P(m|x,z,u) \cdot P(x|z,u)$$

by the chain rule for probabilities.

For simple, local regions, the maximum-likelihood map can be estimated incrementally given knowledge of x and z, so we really just need to solve for $P(x|z,u)$. Additionally, we are not concerned with the full distribution over pose trajectories, as we are updating the map from the maximum-likelihood pose at each time step. Thus, for our online metrical mapping we only need to determine the distribution over the current pose.

$$\begin{aligned} Bel(x_t) &= P(x_t|z_{0:t},u_{1:t}) \\ &= \eta\, P(z_t|x_t,m) \int P(x_t|x_{t-1},u_t) Bel(x_{t-1})\, dx_{t-1}, \end{aligned}$$

where η is a normalization constant. Figure 7 illustrates the basic structure of Markov localization [Fox et al., 1999], which allows us to determine in an efficient and incremental algorithm, the distribution of poses that best fit the current map.

Though multiple metrical mapping methods might be used for the LPM, we utilize the well-known occupancy grid representation [Moravec, 1988; Elfes, 1989], along with particle filter Markov localization [Fox et al., 1999] to overcome noisy odometry information. Stated more plainly, we model the world as a discretized grid, where each cell contains a probability of being occupied by an obstacle, as measured by a lidar sensor. Localization is performed by comparing hypothesis poses to the current map, and the map is updated accordingly. This is a well-known version of simultaneous localization and mapping (SLAM) [Thrun et al., 2005]. Discussions in this paper that refer to this implementation generalize to many SLAM implementations.

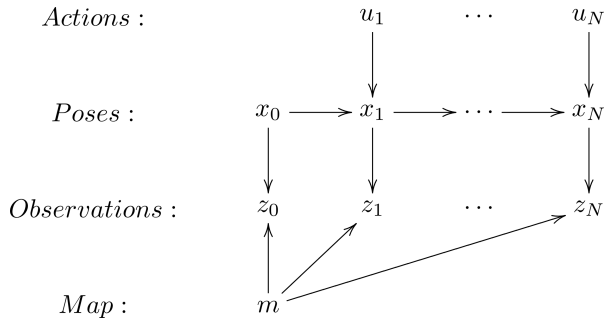

Figure 7: **Markov localization.** The standard graphical dynamic Bayesian network (DBN) for Markov localization within a single frame of reference: combines belief about actions $P(x_t|u_t, x_{t-1})$ and observation $P(z_t|x_t, m)$. Simultaneous localization and mapping (SLAM) algorithms combine localization, $P(x|z,u)$, with one of a number of mapping methods to estimate $P(x, m|z, u)$.

4.2 LPM Benefits

LPMs provide the HSSH with various information that allows both local and global abstractions of space. In Section 5, we discuss how the LPM supports the abstraction of a symbolic small-scale space description of the local-paths in the surround. Section 7 discusses how the local metrical information is used, along with the topological map, to find the global metrical place layout of an exploration trace and, if desired, the entire global metrical map of an explored environment. We forgo these details here; however, the LPM is also useful for local control at the SSH Control Level.

Given a target pose in the LPM, the robot can compute a trajectory to reach the target without colliding into obstacles. This can be done using the Vector Field Histogram [Borenstein and Koren, 1991], the Dynamic Window approach [Fox et al., 1997], gradient methods [Konolige, 2000], or even a simple search (using A* or RRTs [Kuffner and LaValle, 2000]) over the cells of the occupancy grid. The potential function (for gradient methods) or the cost function (for A*) reflects the distance of the agent from an obstacle or other hazard represented in the LPM. Object tracking may be implemented at this level, but our current robot implementation simply avoids obstacles by taking the first few steps along the planned trajectory before replanning. We discuss the selection of target poses as they apply to Causal Level *Travels* and *Turns* in Section 5.3.

In the basic SSH [Kuipers, 2000], an agent localizes itself in a place neighborhood by hill-climbing to a distinctive state. Localization by physically moving to maximize a "distinctiveness measure" requires very little knowledge about the nature of the environment or the sensors. In the Hybrid SSH, on the other hand, the agent uses an online SLAM method to localize itself unambiguously within the local perceptual map. SLAM methods depend on stronger knowledge about the relation between sensor input and the agent's location in the local frame of reference—$P(z_t|x_t, \tilde{m})$. In return for these stronger assumptions, the agent does

not need to move to a particular location to be adequately localized.

Finally, when the agent is in the neighborhood of a particular topological place p, a snapshot of the LPM $\tilde{m}$ serves as a small-scale space description of the place neighborhood that is stored as a place annotation m_p in the topological map. When a place p is first encountered, the local map m_p for its neighborhood is initialized with the information from the scrolling map $\tilde{m}$. The frame of reference defined for m_p may be different from that of $\tilde{m}$, appropriate to the characteristics of the place neighborhood. When the neighborhood of p is encountered on subsequent occasions, the agent may localize itself with respect to the stored map m_p and may update m_p with the more recent information in $\tilde{m}$.

5 HSSH Local Topological Level

As the robot and its scrolling LPM move continuously through the environment, the robot identifies a discrete set of isolated *places* and the *path segments* that connect them. In the small-scale space of the LPM, a place neighborhood is an extended region. In the large-scale space representation, a place is a node in the topological graph, and is connected by paths to other places. These are the local elements from which a global topological map is constructed. We abstract the structure of a place neighborhood to the *local topology* description of the place. Just as a path describes the linear order of places on it, a place describes the circular order of directed paths radiating from it. We call this the local topology S_p of a place p, and describe the circular order with a structure called a *star* [Kuipers et al., 2004]. This section discusses how this symbolic representation of a place (in large-scale space) is grounded in the metrical description m_p of the place neighborhood (in small-scale space).

A *local-path* $\tilde{\pi}$ at a place p is the fragment of a topological path that is visible within the stored local perceptual map, m_p, of the neighborhood of p. A *directed local-path* is of the form $\tilde{\pi}^d$, where $d \in \{+,-\}$ represents the direction along $\tilde{\pi}$ moving away from p. Upon arriving at a new place, a local-path and its directions may not yet have been matched with a global topological path and its directions.

A *star* S is a set of directed local-paths such that $\tilde{\pi}^+ \in S \iff \tilde{\pi}^- \in S$. There are two functions that describe stars.

- $next:\ S \to S$ induces a clockwise circular order over $\tilde{\pi}^d \in S$. $next(\tilde{\pi}^d)$ is the next element from $\tilde{\pi}^d$ in the clockwise order.
- $\alpha:\ S \to \{0,1\}$ associates an attribute value $\alpha(\tilde{\pi}^d)$ to $\tilde{\pi}^d \in S$, where $\alpha(\tilde{\pi}^d) = 1$ means that travel is possible along $\tilde{\pi}^d$ away from p, and $\alpha(\tilde{\pi}^d) = 0$ means that travel away from p along $\tilde{\pi}^d$ is not possible.

The star is naturally encoded as a sequence of pairs, where the sequence encodes the *next* relation (*next* of the last element being the first element), and the second element of each pair is the value of α applied to the

first element. For example, consider the following local topology (star) descriptions of familiar intersection types[6] including local-paths $\tilde{\pi}_a$, $\tilde{\pi}_b$, and sometimes $\tilde{\pi}_c$. (For ease of visualization, the first directed local-path in the circular order is the one directed upward.)

$$
\begin{array}{ll}
+ & [\langle\tilde{\pi}_a^+,1\rangle,\langle\tilde{\pi}_b^+,1\rangle,\langle\tilde{\pi}_a^-,1\rangle,\langle\tilde{\pi}_b^-,1\rangle] \\
\mathsf{T} & [\langle\tilde{\pi}_a^-,0\rangle,\langle\tilde{\pi}_b^+,1\rangle,\langle\tilde{\pi}_a^+,1\rangle,\langle\tilde{\pi}_b^-,1\rangle] \\
\mathsf{L} & [\langle\tilde{\pi}_a^+,1\rangle,\langle\tilde{\pi}_b^+,1\rangle,\langle\tilde{\pi}_a^-,0\rangle,\langle\tilde{\pi}_b^-,0\rangle] \\
\mathsf{Y} & [\langle\tilde{\pi}_a^-,0\rangle,\langle\tilde{\pi}_b^+,1\rangle,\langle\tilde{\pi}_c^-,0\rangle,\langle\tilde{\pi}_a^+,1\rangle,\langle\tilde{\pi}_b^-,0\rangle,\langle\tilde{\pi}_c^+,1\rangle] \\
\mathsf{K} & [\langle\tilde{\pi}_a^+,1\rangle,\langle\tilde{\pi}_b^+,1\rangle,\langle\tilde{\pi}_c^+,1\rangle,\langle\tilde{\pi}_a^-,1\rangle,\langle\tilde{\pi}_b^-,0\rangle,\langle\tilde{\pi}_c^-,0\rangle] \\
\psi & [\langle\tilde{\pi}_a^+,1\rangle,\langle\tilde{\pi}_b^+,1\rangle,\langle\tilde{\pi}_c^-,0\rangle,\langle\tilde{\pi}_a^-,1\rangle,\langle\tilde{\pi}_b^-,0\rangle,\langle\tilde{\pi}_c^+,1\rangle]
\end{array}
$$

An *isomorphism* $\phi : S \rightarrow S'$ between two stars S and S' is a bijective function such that

$$
\begin{aligned}
next(\phi(\tilde{\pi}^d)) &= \phi(next(\tilde{\pi}^d)) \\
\alpha(\phi(\tilde{\pi}^d)) &= \alpha(\tilde{\pi}^d) \\
path(\phi(\tilde{\pi}^d)) &= path(\phi(\tilde{\pi}^{opp(d)})),
\end{aligned}
$$

where $path(\tilde{\pi}^d) = \tilde{\pi}$. An isomorphism means that the two stars have the same local topology under a suitable rotation of the circular order. Note that two stars may have multiple distinct isomorphisms. For example, there are four distinct isomorphisms between two + intersections.

The local topology description provides a purely qualitative account of "left" and "right", avoiding the need to define them in terms of thresholds on some angular variable. A particular directed local-path at a place p, $\tilde{\pi}^+$, and its opposite, $\tilde{\pi}^-$, partition the other directed local-paths in the star into two groups. Those that are between $\tilde{\pi}^+$ and $\tilde{\pi}^-$ in the clockwise direction can be described as being "to the right" of $\tilde{\pi}^+$. Those between $\tilde{\pi}^+$ and $\tilde{\pi}^-$ in the counter-clockwise direction can be described as "to the left" of $\tilde{\pi}^+$. This also defines the appropriate destination for a route instruction such as "turn right" when the agent is at a place p, facing along a directed path $\tilde{\pi}_a^+$. The pragmatics of natural language requires that "turn right" must uniquely specify a directed local-path $\tilde{\pi}_b^d$ that is "to the right" of $\tilde{\pi}_a^+$, such that $\alpha(\tilde{\pi}_b^d) = 1$ (i.e., $\tilde{\pi}_b^d$ is navigable from p).

5.1 Grounding Local Topology in the Local Perceptual Map

We have illustrated how to describe a place symbolically as a circular order of directed local-paths. Here we discuss how to use *gateways* to ground local-paths in the LPM. Gateways allow the robot to ground

[6]Note that we do not have a fixed set of equivalence classes for local topology abstraction. Though there is an upper bound on the number of paths that can fit into an LPM, this is determined by the path width and the LPM size. Thus, many types of intersections can exist that cannot be "named" using a letter.

large-scale actions in the small-scale metrical models, abstract a symbolic local topology description from the small-scale model, and detect and compare places in the environment.

5.1.1 Gateways

The term "gateway" is adapted from Chown et al. [1995], who define gateways as the locations of major changes in visibility.

> In buildings, these [gateways] are typically doorways.... Therefore, a gateway occurs where there is at least a partial visual separation between two neighboring areas and the gateway itself is a visual opening to a previously obscured area. At such a place, one has the option of entering the new area or staying in the previous area. [Chown et al., 1995, p. 32]

We define a *gateway* as a boundary in the local perceptual map that separates the local place neighborhood from the larger environment. That is, a gateway is the boundary where control shifts between localization within the local place neighborhood and travel from one place neighborhood to another. A gateway has two directions, *inward* (looking into the place) and *outward* (looking away from the place), according to the direction of that shift. The location, extent, and orientation of gateways at a place are saved as annotations of the local place neighborhood map m_p.

In much of human experience with large-scale environments (both natural and man-made) local place neighborhoods are separated from each other (either by boundaries or by distance), and they are connected by travel actions along paths. Navigation in large-scale space is thus typically an alternation between motion along travel paths and motion within place neighborhoods. The existence of gateways, as interfaces between the two types of travel, is therefore a requirement for the abstraction from small-scale to large-scale space. Certainly extreme situations occur, such as place neighborhoods that overlap or are immediately adjacent, or environments with (apparently) no distinctive states at all. These will be discussed in appropriate sections below.

Schröter et al. [2004] and Yeap [1988] discuss finding gateways by looking for occlusions from laser data or local models.[7] Schröter [2006] also details a visual door recognition system for determining gateways. Below, we describe an alternative algorithm for identifying gateways within the small-scale space of the local perceptual map. This algorithm relies on a Voronoi skeleton computed from the free space in the LPM. Our implementation first prunes the Voronoi skeleton, using the fact that we have a bounded LPM to determine the true skeleton of free space in the local surround. It then defines the "core" of the local region by grouping nearby Voronoi junctions, if they exist. Walking along the graph, from the core, to the frontiers of the local map, the algorithm looks for *constrictions* as locations for gateways. Constrictions can be defined several ways, e.g., local minima w.r.t distance to the closest obstacles (what Thrun and Bücken

[7] Gateways are called exits by Yeap [1988]; Yeap and Jefferies [1999].

[1996] called "critical points"). Gateways are then defined as line segments that separate distinct regions of free space in the LPM.

Pruning the Voronoi graph. A Voronoi graph is the set of points equidistant from the two (or more) closest obstacles. It lies on the boundaries of Voronoi regions [Fortune, 1992]. Using a Voronoi graph to describe the free space of a metrical model can be useful; however, given noisy measurements, a Voronoi graph can contain many branches and spurs that do not contribute to the "base" skeleton that describes the "backbone" of the modeled environment. As a result there has been work on pruning of Voronoi graphs [Choset and Nagatani, 2001; Wallgrün, 2005] and on using thinning-based approximations of Voronoi graphs for mobile robot navigation [Choi et al., 2002]. *Thinned skeletons* often have far fewer spurs into concave corners; thus, they represent an approximation of a partially pruned Voronoi skeleton.

In order to determine the "critical" skeleton of a noisy Voronoi graph, we assume that the robot is computing a Voronoi graph in the LPM. Currently, we also remove "island" obstacles by removing occupied or unknown cells in the occupancy grid that are completely surrounded by free cells. This reduces drastic changes in the skeleton due to pedestrians. The Voronoi graph is computed by treating occupied cells in the occupancy grid as obstacles.

Because we use a small, bounded LPM, there is always some region of free space that touches the edge of the occupancy grid or some region of "unknown occupancy" (gray cells in the figures) that may provide an option to leave the current region. We define a terminal point of the Voronoi graph that reaches the edge of the LPM or reaches unexplored cells to be an *exit*. We can then define the branches of the Voronoi graph that contain exits to be "critical" branches. Instead of actively pruning away branches, a better approach is to include only the union of all shortest paths that connect each exit to all other exits in the LPM.[8] Figure 8 shows how this spanning tree eliminates all spurious junctions and branches in these small-scale models.

Determining Gateways. Gateways can be grounded in an LPM by using the Voronoi graph. Though the full, continuous generalized Voronoi graph can be computed vis Fortune's algorithm [Fortune, 1992], it is usually more efficient to approximate the Voronoi graph of an occupancy grid, using pixel-based "brush-fire" algorithms: imagine a brush fire along all defined obstacle pixels, burning inward at a constant speed, and the skeleton is marked by all points where two or more fires meet. Similarly, there exists a thinning algorithm [Zhang and Suen, 1984] that gives a pixel-based skeleton, but with many spurious terminal branches pre-pruned. As both the brush-fire approaches and the thinning approach are linear in the grid size, we utilize the thinned skeleton, as it speeds up the pruning process due to having fewer branches that need to be examined.

Figure 9 shows a few steps of the gateway algorithm on a thinning-based skeleton. The algorithm

[8] Dead-ends are a special case, where only one exit exists. Here we just keep the branch that connects the exit to the Voronoi junction at the dead-end.

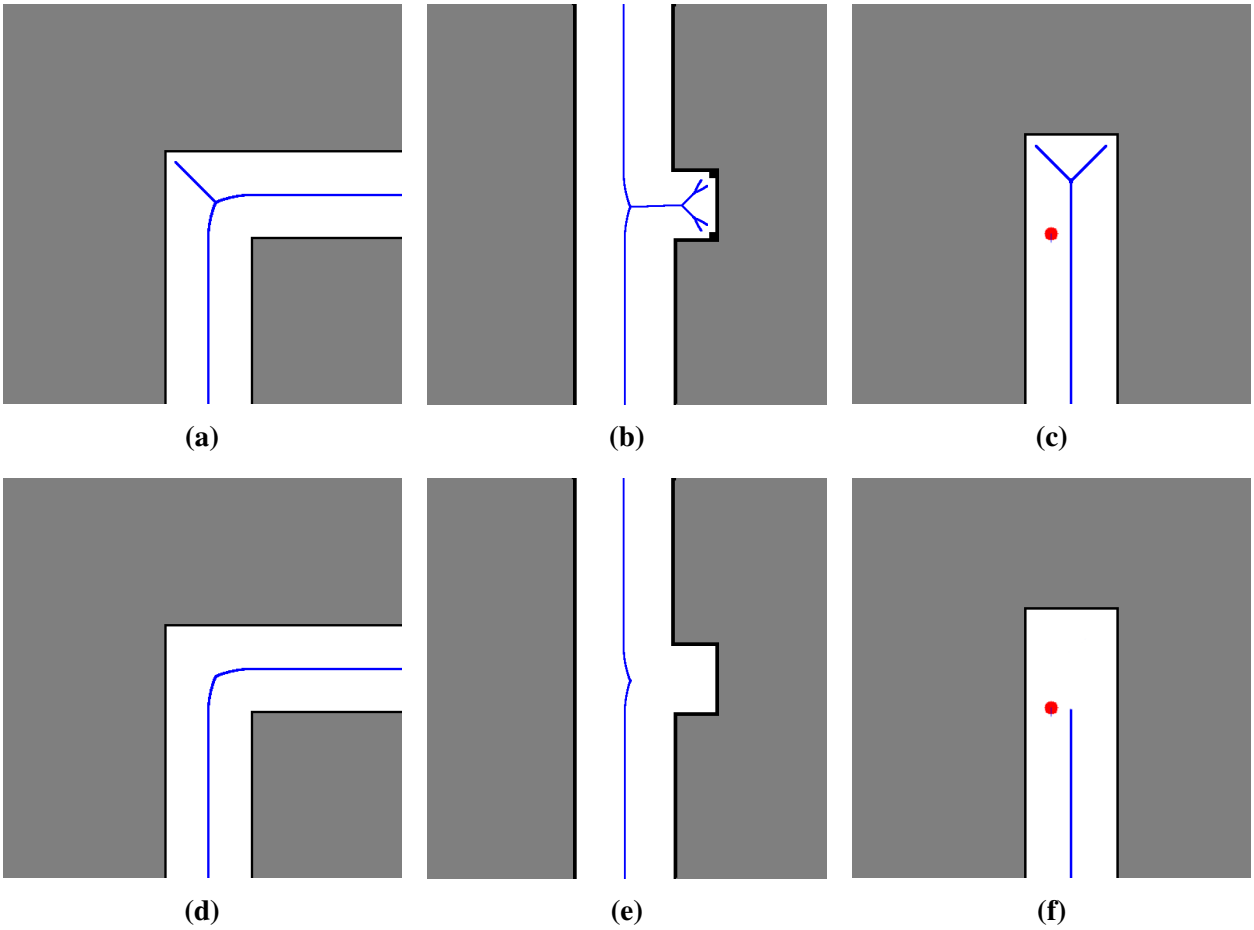

Figure 8: **Pruning a Voronoi graph using the LPM boundary.** **(a,b,c)** Examples of Voronoi graphs at common places. **(d)** Pruning the skeleton at an L leaves no junction, which means methods that rely on junctions in pruned graphs to define places [Choset and Nagatani, 2001] ignore these types of intersections. **(e)** Small bits of noise around objects can cause spurs and hierarchical branches in the Voronoi skeleton. Methods that use fixed-depth or distance-based pruning [Choset and Nagatani, 2001] can leave junctions in the graph, while the LPM pruning eliminates all non-critical branches. **(f)** Dead-ends are a special case where we keep the minimal branch that connects the single exit to the junction closest to the robot.

below has been tested on both thinned skeletons and true Voronoi graphs, and works well on both kinds of skeletons. Given a pruned skeleton, the method for finding gateways is as follows:[9]

- l is the location of the physical robot w.r.t the LPM.
- c is the point on the Voronoi graph closest to l (Figure 9(a)).
- J is the set of Voronoi junctions j (Figure 9(b)).
- r_p is the "Voronoi radius": the distance from Voronoi point p to the closest obstacle.
- $K = \{j \in J : dist(j,l) \leq r_j\}$ (the robot is within the "radius" of the junction point).
- Two junctions j and j' are neighbors if $dist(j,j') \leq max(r_j, r_{j'})$.
- Define the "core" of the place neighborhood as F: the equivalence class of neighboring junctions that includes K as the starting set of junctions. See Figure 9(b).
- If $F = \emptyset$ then define $F = \{c\}$.
- Q is the set of all Voronoi points q, where $\exists f \in F$ s.t. $dist(f,q) = r_f \wedge \forall f' \in F\ dist(f',q) \geq r_{f'}$. This selects the set of points on the border of the "core" of the place.
- For each $q \in Q$, walk along the branch that contains q in the direction away from the "core" of the place (Figure 9(c)). Look for a point p that corresponds to a *constriction*.
- At each of these constrictions m, define a line segment g of length $2 \cdot r_m$, centered on m, oriented normal to the branch at point m. See Figure 9(d).

A recursive version of this algorithm was implemented that runs quickly enough to recompute gateways in real-time (2-3 times a second for a 300x300 cell occupancy grid using an older 450 MHz research robot computer). This implementation was used to produce Figures 9(d), 10(a), 11(a-c), and 12(b,c), and it was the implementation used to detect the places in Figure 15(a). A constriction is currently a local minimum over $r_p \in R$. Defining gateways where the *change in distance* to nearby obstacles is minimal (or plateaus) provides useful gateways at the beginning of hallways and doorways in corridor environments.

We are currently investigating a new algorithm that is a bit more robust: works well given very noisy walls, which can create jagged branches in the Voronoi (and especially in the thinned) skeletons, and handles coastal navigation situations (Figure 11(d)). The new algorithm moves away from looking for constrictions, as they are unreliable in noisy settings and can fail in certain pathological scenarios. Section 9.1 outlines our plans to formally describe and evaluate gateway detection using this improved algorithm.

[9] Symbols used in the discussion of the gateway implementation are local in scope and have no relation to symbols used elsewhere in this paper, even if they are spelled the same.

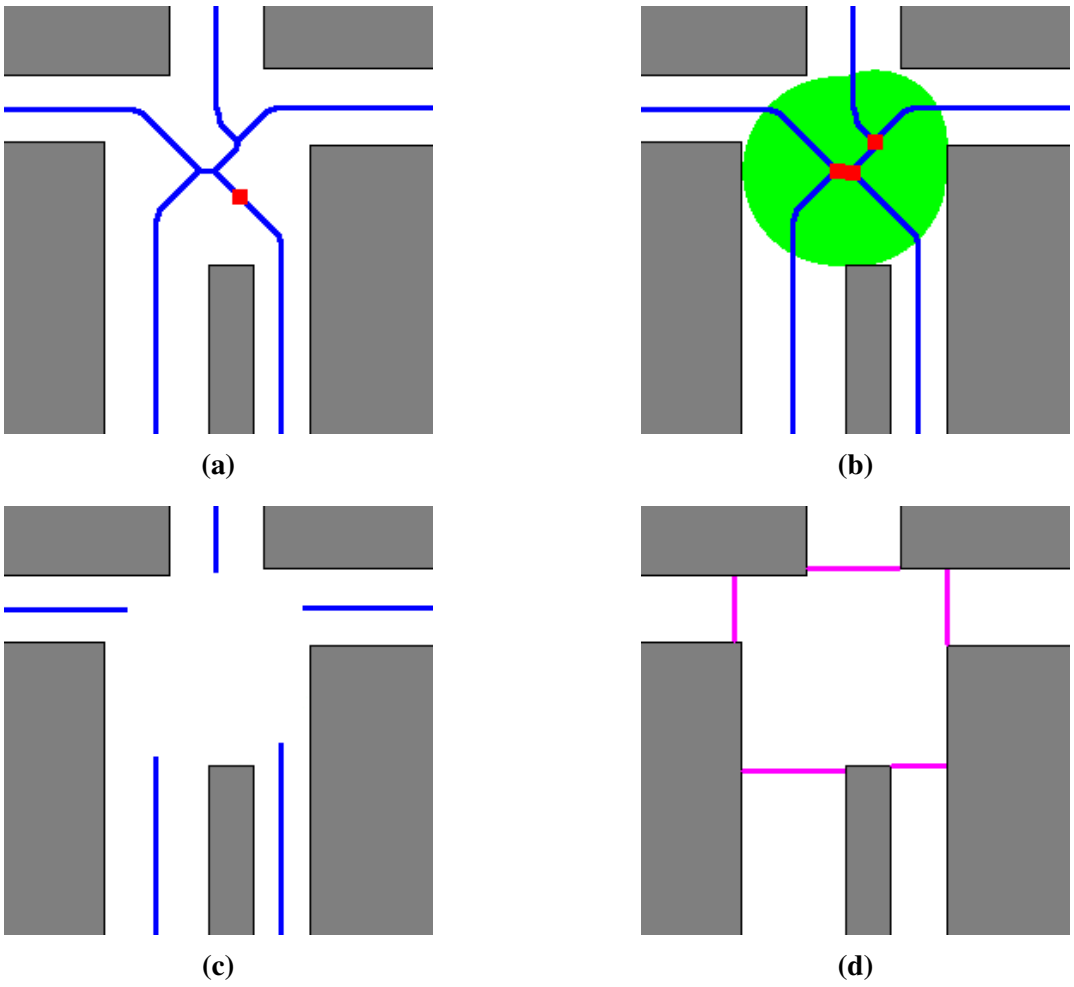

Figure 9: **Example of gateway detection.** Here we show certain steps of the gateway algorithm. We begin with a model of the local surround. **(a)** We then calculate a pruned Voronoi skeleton. Here we use a thinning-based approximation of the Voronoi skeleton [Zhang and Suen, 1984], which we have found to be much faster to calculate on slower processors. We then locate the closest point on the skeleton to the robot. **(b)** The robot then determines the "core" of the local region. **(c)** The algorithm ignores all portion of the skeleton inside of the core, only looking for gateways along portions of the skeleton outside of the core. **(d)** The algorithm looks for a local minimum in the rate of change of the Voronoi radius. These constrictions define the locations of gateways, while the skeleton itself defines the orientation of the gateway.

5.1.2 Local Topology

Given an implementation for detecting gateways in a stored map of a place, m_p, we can ground the local topology concepts of local-paths in our small-scale model of the surrounding environment.

- For each outward-facing oriented gateway $\langle g, out \rangle$, define a *directed local-path* $\tilde{\pi}_g^+$ that leads away from the current place.
- Initialize a circularly ordered *star* S_p with a list (clockwise from an arbitrary starting point) of associations between directed local-paths and oriented gateways, $(\langle \tilde{\pi}_g^+, 1 \rangle \leftrightarrow \langle g, out \rangle)$. Since these are traversable paths, each $\alpha(\tilde{\pi}_g^+) = 1$.[10]
- Test each pair of gateways, g and g', via a *path continuity* test, to determine whether their directed local-paths belong to a single continuous path. If so, give both directed local-paths the same path name (e.g., $\tilde{\pi}_a$ below and in Figures 10(b,c)), and include the inward oriented gateways in the association. For example, change

$$\begin{array}{lcl} (\langle \tilde{\pi}_g^+, 1 \rangle & \leftrightarrow & \langle g, out \rangle) \\ (\langle \tilde{\pi}_{g'}^+, 1 \rangle & \leftrightarrow & \langle g', out \rangle) \end{array} \quad \text{to} \quad \begin{array}{lcl} (\langle \tilde{\pi}_a^+, 1 \rangle & \leftrightarrow & \langle g', in \rangle, \langle g, out \rangle) \\ (\langle \tilde{\pi}_a^-, 1 \rangle & \leftrightarrow & \langle g, in \rangle, \langle g', out \rangle) \end{array}$$

- For each $\tilde{\pi}_g^+ \in S_p$ such that $\tilde{\pi}_g^- \notin S_p$, insert the association $(\langle \tilde{\pi}_g^-, 0 \rangle \leftrightarrow \langle g, in \rangle)$ into the circular order of S_p, in a position determined by its failure of the path continuity test.

In our current implementation, the gateways g and g' belong to a single continuous path if: (1) a ray normal to the orientation of gateway g and centered at the midpoint of gateway g intersects the line segment that defines gateway g'; and (2) vice versa for a ray from g' towards gateway g. (Note that the failure of this test should determine a pair of gateways that the non-traversable path continuation falls between.)

At this point, the star S_p is a complete representation of the local topology of the neighborhood described by the LPM. Since this representation is expressed completely in terms of small-scale space (the gateways g and the directed local-paths $\tilde{\pi}_g^d$), we refer to this as the *small-scale star* (Figure 10(c)). Binding the directed local-paths to directed paths in the topological map of large-scale space implies the appropriate *large-scale star* (Figure 10(d)). This binding is part of the HSSH topological mapping process, and is discussed in Section 6.1.

[10] In future implementations, $\alpha : S \rightarrow \{\text{MIDLINE}, \text{LEFTWALL}, \text{RIGHTWALL}, \text{DEADEND}, \text{NONE}\}$ should associate directed local-paths with attributes representing the control laws for traversing the path in that direction. (LEFTWALL and RIGHTWALL imply coastal navigation scenarios. For terminating local-paths, DEADEND means that further travel is blocked, while NONE means that no control law is applicable.)

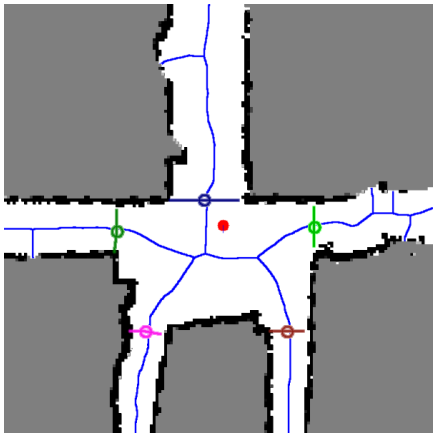

(a)

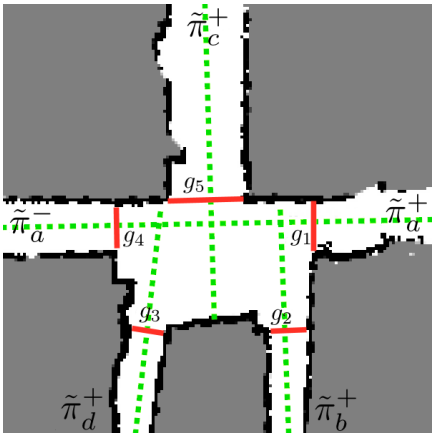

(b)

Small-scale star description

$$
\begin{array}{lcl}
(\langle \tilde{\pi}_a^+, 1\rangle & \leftrightarrow & \langle g_4, in\rangle, \langle g_1, out\rangle) \\
(\langle \tilde{\pi}_b^+, 1\rangle & \leftrightarrow & \langle g_2, out\rangle) \\
(\langle \tilde{\pi}_c^-, 0\rangle & \leftrightarrow & \langle g_5, in\rangle) \\
(\langle \tilde{\pi}_d^+, 1\rangle & \leftrightarrow & \langle g_3, out\rangle) \\
(\langle \tilde{\pi}_a^-, 1\rangle & \leftrightarrow & \langle g_1, in\rangle, \langle g_4, out\rangle) \\
(\langle \tilde{\pi}_d^-, 0\rangle & \leftrightarrow & \langle g_3, in\rangle) \\
(\langle \tilde{\pi}_c^+, 1\rangle & \leftrightarrow & \langle g_5, out\rangle) \\
(\langle \tilde{\pi}_b^-, 0\rangle & \leftrightarrow & \langle g_2, in\rangle))
\end{array}
$$

(c)

An example large-scale star abstraction

$$
\begin{array}{lcl}
((\langle \pi_1^+, 1\rangle & \leftrightarrow & q_1) \\
(\langle \pi_2^+, 1\rangle & \leftrightarrow & q_2) \\
(\langle \pi_3^-, 0\rangle & \leftrightarrow & q_3) \\
(\langle \pi_4^+, 1\rangle & \leftrightarrow & q_4) \\
(\langle \pi_1^-, 1\rangle & \leftrightarrow & q_5) \\
(\langle \pi_4^-, 0\rangle & \leftrightarrow & q_6) \\
(\langle \pi_3^+, 1\rangle & \leftrightarrow & q_7) \\
(\langle \pi_2^-, 0\rangle & \leftrightarrow & q_8))
\end{array}
$$

(d)

Figure 10: **Identifying gateways and local topology in the LPM.** The local perceptual map (LPM) is implemented as a bounded occupancy grid. The robot is shown as a circle in the center of the LPM. **(a)** The gateways separating the core from the exits are defined. In our implementation this is done using a pruned Voronoi skeleton. **(b)** Gateway locations and directions are used to identify the directed local-paths and to determine which pairs satisfy the path continuity requirements. **(c)** The small-scale star enumerates directed local-paths in clockwise order, describing their traversability and association with gateways. Note: the robot entered the place via g_5; thus, it arrived on directed local-path $\tilde{\pi}_c^-$. **(d)** The large-scale star (Section 6.1) replaces local-paths with topological paths from the global topological map, and defines a distinctive state for each directed path at this place. This environment has five gateways, four paths, and eight distinctive states.

5.2 Detecting Places

To explain local topology extraction, we provided examples where the robot was already at a place. Perhaps surprisingly, the method for constructing the local topology of a place neighborhood does not actually depend on being at a place neighborhood. Gateways can also be defined along paths, as they separate the robot from the "frontier" of the LPM. Therefore, if we recalculate gateways and local topology at each time step, we can very easily *detect* places.

We define the robot to be *on-path* when the local topology of the LPM contains exactly two gateways and exactly one path (e.g., Figure 11(a)). When the agent is on-path, it is selecting and executing control laws (and hence primitive motions) to perform a travel action. The LPM scrolls as the agent moves, keeping the agent near its center cell, and serving as an observer for the local small-scale space.

When the agent is not on-path, it is in a place neighborhood. In this situation, the agent establishes a fixed correspondence between the LPM and the structure of the place neighborhood. Here, the LPM serves as a local metrical map m_p of the place neighborhood (and does not scroll with the agent's motion within the place neighborhood). Thus, the number and location of places in an environment depends in part on the predetermined size of the LPM[11], though places are not sensitive to small changes in LPM size.

When the robot is not on-path, it either has more than one local-path, which occurs at intersections or open doorways, or one local-path with only one gateway, which occurs at dead ends. These are all places (Figure 11). There is a degenerate case where no gateways exist. Due to our implementation of gateways, this situation means there is no way out of the current location, so the robot's entire world is simply modeled by a single place and LPM.[12]

When traveling along a path, the robot may see multiple unaligned gateways and suspect it is at a place. Sometimes, false gateways appear in the LPM due to the boundary between observed free space (i.e., white cells in the occupancy grid) and unknown space (i.e., gray cells in the grid). This is often the case when the robot's sensors do not provide a 360° field of view, as with SICK-brand lidars. Before the robot commits itself to being at a place, it must perform some local exploration in the fixed map of the potential place to eliminate any false gateways. We have found that for a robot with a 180° field of view, simply rotating in place eliminates most false gateways.

Using the local topology defined by gateways allows the robot to detect places more reliably than when using methods that simply look for Voronoi graph junctions. First, Voronoi graphs can have many spurious junctions. This is especially true given noisy sensors or environments, but even occurs in the face of no noise at small alcoves and other common architectural features. Similarly, complex intersections can have multiple junctions. The gateways and local topology can see one place, whereas a junction-based approach

[11] One interesting avenue of future research is to try adapting the LPM size by environment characteristics.

[12] There is another degenerate case when the robot is in the middle of a featureless environment. As mentioned in Section 3.5, the HSSH currently does not handle these types of environments.

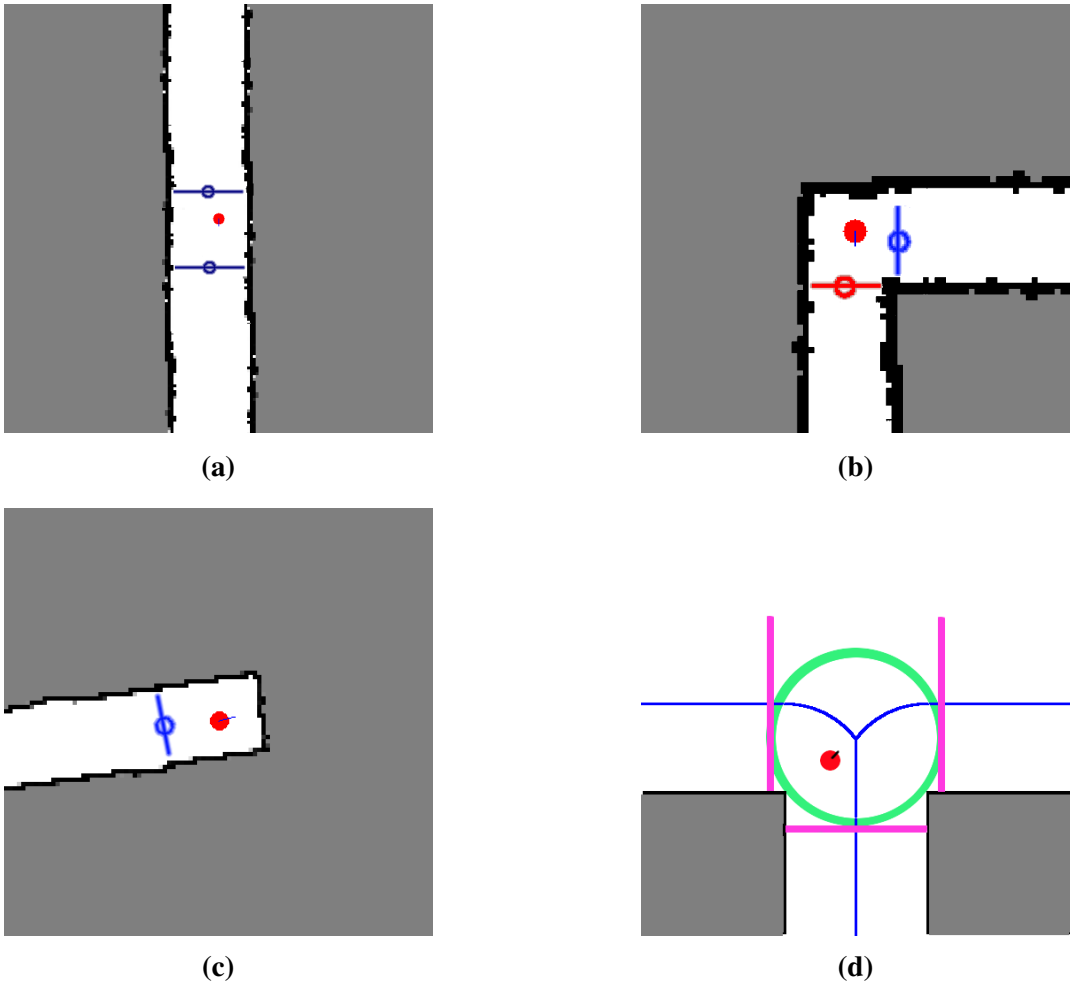

Figure 11: **More real-world gateways.** Our current gateway algorithm uses a Voronoi skeleton to find the gateways surrounding a location. **(a,b)** Even at locations with no Voronoi junction points, the gateway algorithm works. Example (a) shows the robot on a path, where two gateways on either side of the robot give a stable topology, and (b) shows the robot at a place. **(c)** At dead ends, there is only a single gateway. **(d)** The gateway algorithm is being generalized to handle skeletons in both midline and coastal navigation situations. This uses the extended Voronoi graph (EVG) [Beeson et al., 2005].

(including Delaunay triangle approaches [Silver et al., 2004]) must define multiple strangely connected places. Figures 9(b) and 10(a) both show multiple junctions at a single place. Additionally, there exist important places detected via the gateway approach, like L intersections, that contain no junctions at all after pruning the Voronoi graph (Figures 8(d-f)).

5.3 Selecting Local Motion Targets

Instead of relying on the dynamical system approach to motion used in the basic SSH, we introduce gateways as an alternative approach. Gateways provide a geometric method for control of motion—where midline or coastal navigation along paths is applicable. The motion of the robot in large-scale space can be adequately captured by noting which oriented gateways the robot passes through. Reconsider the example of abductive inference for a topological map in Figure 4 that modeled the world as points connected by lines. Compare this to the Hybrid SSH approach illustrated in Figure 12 where turns and travels correspond to moving towards gateways.

As discussed in Section 4.2, local motion planning consists of selecting a target pose in the LPM, computing a safe trajectory to it, executing the first step of that trajectory, sensing the environment, updating the LPM, and repeating the cycle. The selection of target poses for local motion control corresponds to the action or goal being pursued. There are three distinct cases.

- If the agent is not in a place neighborhood, it is *on-path*, in which case it is moving along the local-path in the LPM toward one of the two gateways. Just beyond the forward gateway, in the outward orientation, is an appropriate target for local motion planning; however, a more robust approach with respect to obstacle avoidance is to aim at a point well beyond the gateway, like the edge of the LPM. As the LPM scrolls, the gateway location is constantly refreshed. The robot never reaches the gateway until its location becomes stable (which only happens when the agent arrives at a place).[13]

- If the agent is in a place neighborhood, the LPM is fixed to the local environment, so motion planning is confined to the small-scale space of the place neighborhood. The agent may have a pragmatic destination within the place neighborhood, for example an intelligent wheelchair may have the goal of bringing its driver to her desk after entering her office, in which case the local motion target is a pose associated with that destination. Such motion targets can also be generated when exploring the fixed LPM of a potential place.

- The agent may be executing a turn action as part of a route through large-scale space. In this situation, the LPM is fixed in the local frame of reference, and a large-scale turn action corresponds to moving from an inward-facing oriented gateway to a location just beyond an outward-facing oriented gateway.

[13] Lee [1996] calls control algorithms that continuously re-plan for a moving point ahead as "red wagon" controllers.

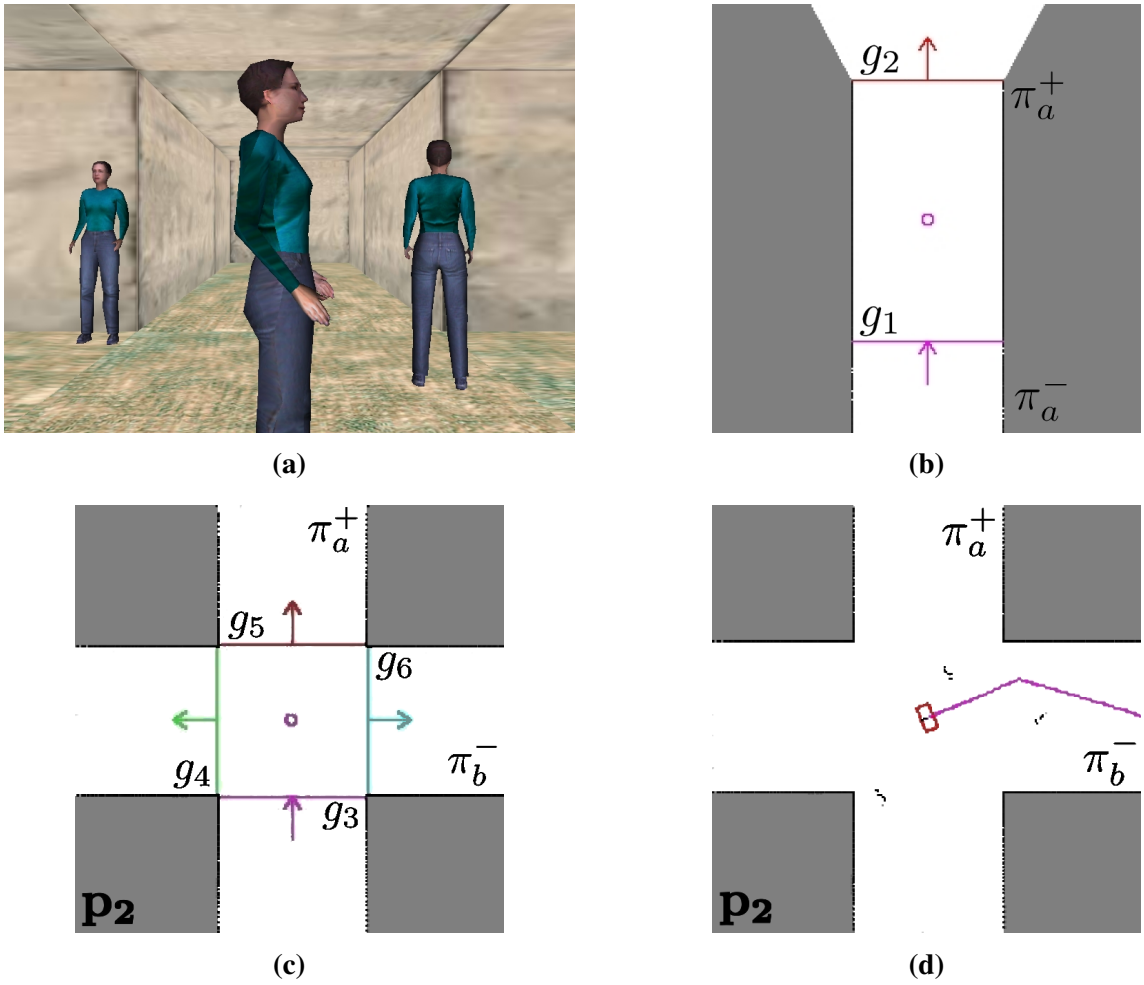

Figure 12: **Grounding control using gateways.** **(a)** The example from Figure 4 is further examined in a simulated 3D office environment with obstacles. The gateways are found and drawn on the LPM in real-time, with arrows representing the outward orientations that leave the current area. The gateway associated with the robot's past motion is depicted using an arrow pointing in the inward orientation. **(b)** Traveling along directed path π_a^+ corresponds to aiming for an oriented gateway, e.g., $\langle g_2, out \rangle$, in the appropriate direction. The gateway is continually recomputed, which keeps moving the local motion target along the path, until it becomes stable at the entrance to a place. **(c)** Arriving at dstate q_2 at place p_2 corresponds to arriving at a gateway $\langle g_3, in \rangle$ associated with a directed local-path $\tilde{\pi}_a^+$ in the LPM for place p_2. The turn action from dstate q_2 to q_3 corresponds to local motion within the LPM through outward-facing oriented gateway $\langle g_6, out \rangle$ on directed local-path $\tilde{\pi}_b^-$. **(d)** In calculating local topology, "island" obstacles that are surrounded by free space are removed to ensure reliable gateway detection. Planning to move through a gateway requires consideration of these obstacles. Once the robot moves past gateway $\langle g_6, out \rangle$, two new aligned gateways appear that will flank the robot throughout the next travel action, as in image (b).

After passing through the outbound gateway, the robot is in position to begin following another path. Note, that the TurnAround action simply corresponds to traveling past the same gateway the robot entered the place through, facing the outward instead of the inward orientation. Continuing along a path that passes through a place (no turn) also falls into this case.

In certain scenarios, such as two large rooms connected by a doorway, it may be possible for an agent to move directly from one place neighborhood to another, moving between two distinct local topologies, without ever being significantly *on-path*. The SSH can accommodate this transition with a dummy travel action whose effect is simply to transition between the reference frames of two adjacent, or even slightly overlapping, places.[14]

6 HSSH Global Topological Level

The next two sections will address the problems of building a global topological map to describe the qualitative structure of large-scale space and building a global metrical map to describe its geometric structure within a single global frame of reference. We describe these two map-building problems separately, but their solutions benefit from each other and should be interleaved in future research (Section 9.2).

The first problem is to identify the best global topological map consistent with exploration experience. The process of generating possible topological maps from experience and testing them for consistency can provide formal guarantees that the correct map is generated and never discarded [Dudek et al., 1993]. A logic-based theory of topological maps [Remolina and Kuipers, 2004] makes explicit the assumptions upon which those guarantees depend.

If the robot knows it is in an environment with no loops, creating a topological map is quite easy. This is especially true given deterministic actions, as the robot simply moves deterministically between known places when it revisits parts of the environment. Even with non-deterministic actions, creating the topology of such environments is still possible [Tomatis et al., 2002]. The difficulty in map-building arises from closing loops: determining when a newly-encountered place is the same as a previously-experienced place, and creating a hypothesized new loop in the topological map. When large loops in the environment result in structural ambiguity, a topological representation can concisely represent the loop-closing hypotheses by generating a single topological map for each qualitatively distinct alternative.

[14] Taking this idea to an extreme, the Atlas system [Bosse et al., 2003] creates new frames of reference based on feature counts, building a "patchwork" map of overlapping frames of references. However, if the entire environment is described in terms of overlapping place neighborhoods, the benefit of the topological map as a concise description of large-scale space is decreased. Likewise, the local and global distinctiveness of places is sacrificed.

6.1 From Small-Scale to Large-Scale Star

In small-scale space, the LPM is used for the detection of gateways, local-paths, and places, and to create the local map m_p that is stored at places. The small-scale star describes both a circular order on the set of directed local-paths in a place neighborhood and also the correspondence between directed local-paths and oriented gateways. A place p in large-scale space is associated with the local map m_p, a model of the place neighborhood in small-scale space. At a place, each directed local-path $\tilde{\pi}^d$ in small-scale space corresponds to a directed path π^d in large-scale space. This allows us to determine the large-scale star that describes the circular ordering of topological directed paths at the place.

Assimilating the local topology of a place into the global topological map requires a 1-1 mapping between the directed local-paths in the small-scale star and a set of directed paths from the global topological map. In Figures 10(c,d), we illustrate such a mapping between the local-paths, $\tilde{\pi}_a$, $\tilde{\pi}_b$, $\tilde{\pi}_c$, and $\tilde{\pi}_d$, and the corresponding global topological paths π_1, π_2, π_3, and π_4, respectively. To keep this example simple, we specified $+$ and $-$ on the directed paths to correspond consistently, but of course this need not be true in general.

In large-scale space, a distinctive state q corresponds uniquely to a place, a path, and a direction on that path (Equation 1). Thus, the dstate q is at a particular place p, and there is a bijective association between a dstate and a directed local-path: $\psi_p(q) = \tilde{\pi}^d$ where $\tilde{\pi}^d \in S_p$. This implies that in the case where the directed local-path passes through the place, the distinctive state q will correspond with two different oriented gateways, one $\langle g, in \rangle$ entering the place neighborhood, and the other $\langle g', out \rangle$ departing from it.

An isomorphism $\phi : S \rightarrow S'$ between two stars implies a bijective mapping between the associated dstates as well. We will extend ϕ to write these implied mappings as $\phi(q) = q'$. For a topological map M^T, and the set P of places in M^T, we can now define the set of local place maps,

$$M^P = \{\langle p, m_p, S_p, \psi_p \rangle \ : \ p \in P\}$$

associating each place $p \in P$ with its local metrical map m_p, its local topology S_p, and ψ_p, the association between dstates and directed local-paths in the local topology.

Assuming that the LPM is sufficiently well explored, the set of directed local-paths and gateways in the small-scale star is complete, so the description of the distinctive states and directed paths in the circular order of the large-scale star is also complete. A *turn* action in large-scale space corresponds to motion in small-scale space within a place neighborhood from the inward-facing oriented gateway the robot arrived upon to an outward-facing oriented gateway (Figure 12(c)). Thus, for every pair of dstates q_i and q_j at the place, a causal schema for the turn action $\langle q_i, turn, q_j \rangle$ is implicitly defined. Exploration experience can now be described as an alternating sequence of travel actions and place neighborhoods, which simplifies construction of the global topological map (Figure 5).

6.2 The Tree of Possible Topological Maps

The topological map-builder maintains a tree whose nodes are pairs $\langle M, q \rangle$, where M is a topological map (augmented below for the HSSH) and q is a distinctive state within M representing the robot's current position. The leaves of the tree represent all possible topological maps consistent with current experience [Dudek et al., 1993]. The algorithm for growing the tree of possible topological maps was presented in Figure 5. This figure also describes the differences between map-building in the basic SSH and Hybrid SSH.

After each action a and resulting view v, we extend each map hypothesis at a leaf of the tree. If the current action moves within known territory, the map $\langle M, q \rangle$ will predict the resulting dstate q' and the view to be observed, so the hypothesis can be updated or refuted according to whether the prediction was correct or not. If the current action explores new territory, then either the resulting dstate is also new, or the action closes a loop and connects with a previously known dstate. Since there may be multiple possibilities that all match view v, the tree of topological map hypotheses will branch. For purposes of generating and testing candidate topological maps in the HSSH, we will extend the basic SSH topological map M^T with $M^P = \{(p, m_p, S_p, \psi_p) \ : \ p \in P\}$, the set of local metrical maps and local topologies of individual place neighborhoods.

$$M = \langle M^T, M^P \rangle$$

In the SSH, a view v is an abstracted description of the agent's perception of the local environment from a distinctive state q. We select the level of description to ensure that the view is a deterministic function of the dstate ($v = o(q)$), although we allow perceptual aliasing (different states with the same view) [Kuipers and Beeson, 2002]. In the basic SSH, a view is a symbol, abstracting away the nature of the perceptual system, and views are matched only for equality. In the Hybrid SSH, we define a view to be the local topology S_p of the current place p and the current directed local-path the robot is on; thus, the new view description is derived from the local topology, which is grounded in local perceptual map m_p.

$$\begin{aligned} v &= \langle S_p, \tilde{\pi}^d \rangle \text{ where } d \in \{+, -\} \\ &= \langle S_p, \psi_p(q) \rangle \end{aligned}$$

Given two views v and v', we say that $match(v, v')$ holds iff there is an isomorphism $\phi : S \rightarrow S'$ such that $\phi(q) = q'$. That is, from the perspectives of the specified dstates, the local topologies match.

As exploration progresses, the map M is extended with new information. For example, after an exploration step that closes a loop in the map, the resulting map M' is M extended with a new dstate q' and assertions $\langle q, a, q' \rangle$, $v = o(q')$, and $q' = q_j$. A new version of $M^C = \langle Q, A, V, S, o \rangle$ is created, and the implications of the loop-closing assertion $q' = q_j$ propagate through new versions of M^T and M^P to unify place

and path labels as necessary. Because we are matching complete local topologies in the HSSH, the tree of maps only branches on travel actions. Turn actions are already fully described by the large-scale star.

6.3 Topological Mapping Example

We applied an implementation of the Hybrid SSH map-builder to an exploration of an office environment with multiple nested large loops. This office had a large number of cubicles and office doorways. To respect student and faculty privacy, we prune the Voronoi skeleton so that Voronoi branches, thus gateways, were defined only for large hallway intersections, not at doorways or cubicle openings. The environment, as defined by the robot, contained 6 paths and 9 places with 4 distinct local topologies. Figure 13 shows the exploration route as a sequence of place visits, the sequence of LPMs observed at successive place neighborhoods, and the unique simplest topological map that resulted from the mapping algorithm, with LPMs overlaid at corresponding places in the correct topological map.

After an exploration consisting of 14 travel actions, the topological mapper finds 83 possible configurations of the environment that are consistent with the observed local topologies and the topological axioms—that is there exist 83 leaves in the tree of maps. The prioritized circumscription [Remolina and Kuipers, 2004] on this set of maps produces 4 minimal models. All but one of these can be eliminated with further exploration or by simply matching LPMs using the alignments specified by the four minimal maps. This final map model is the correct topological representation of the environment.

If we assume planarity of the environment, we can use a more sophisticated version of the topological map-building algorithm [Savelli and Kuipers, 2004] that rules out many more models as inconsistent. Here, there are only 46 consistent configurations of the exploration experience, and the circumscription policy produces a single minimal model, which is the correct topological map of the environment (Figure 13(c)). Currently, our implementation can build the complete tree of maps for this exploration trace and determine the unique minimal map of this environment in $\sim$200 ms on the robot's Pentium III 450 MHz processor. Notably, the results presented on this office environment would be unchanged if the path segments were longer or even very convoluted, as the number of places and paths would not change. Additionally, the tree of maps ensures the correct map is never discarded.

The complexity of the map computation is the following. Let n be the number of poses in the exploration trajectory; let m ($m \ll n$) be the number of topological places; let k ($k < m$) be the maximum number of places matching an observed view; and let l be the maximum number of directed local-paths in the local topologies (often $l \leq 4$). For example, for the environment in Figure 13, $n \approx 7300$, $m = 9$, $k = 4$, and $l = 4$. The maximum branching factor in the tree of maps is $k+1$. Branches only occur when the robot travels between two connected places for the first time, which can only happen at most $ml/2$ times. This means the size of the tree of maps is $O(k^m)$; thus, computing the tree of maps is exponential in m (not in n). The exponent decreases by at least a factor of 3 compared with the basic SSH version due to branching only

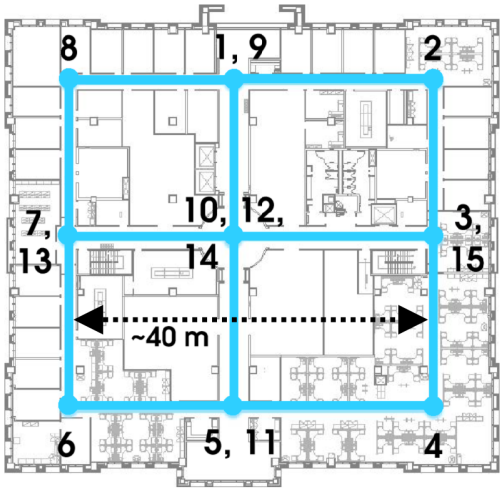

(a)

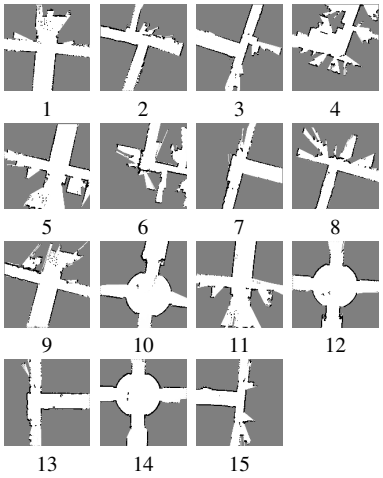

(b)

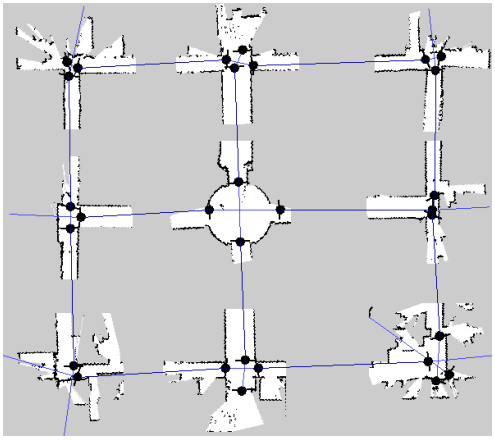

(c)

Figure 13: **An environment with multiple nested loops.** In the CAD drawing **(a)**, we show the path traveled between places in the environment. We enumerate the order of places in the exploration taken by the robot. (This exploration trace was also used for Figure 1.) In **(b)**, we show the LPMs created at the places during the travel. We constrained the gateway algorithm in order to ignore open office doors and cubicle openings, which ensures places only at hallway intersections. The stars generated from these LPMs are used to search through the space of consistent topological maps. In **(c)**, we show the unique topological map generated after matching local stars and LPMs. The map is overlaid with the LPMs generated at the places, with the gateways, and with the connections between gateways which lie on the same path.

on travels, not on turns, and matching local topologies of places.[15] Savelli and Kuipers [2004] also show that the planarity constraint gives an additional improvement in the branching factor k by rejecting many loop-closing hypotheses.[16]

6.4 Levels of Spatial and Temporal Granularity

At this point, we summarize the three different levels of granularity, with different ontologies, that we are using to describe space and time.

The agent's experience is a trajectory through the environment. At the SSH Control Level and in the LPM, the trajectory is represented using a fine-grained representation for time t, pose x, motor signal u, and sensory image z. These are used both for control laws, and for simultaneous localization and mapping to build the LPM. Expanding Figure 7, the agent's exploration experience is described by

$$\begin{array}{ccccccccccccc}
 & & \cdots & & u_{t-1} & & u_t & & u_{t+1} & & \cdots & & u_N \\
 & & & & \downarrow & & \downarrow & & \downarrow & & & & \downarrow \\
x_0 & \rightarrow & \cdots & \rightarrow & x_{t-1} & \rightarrow & x_t & \rightarrow & x_{t+1} & \rightarrow & \cdots & \rightarrow & x_N \\
\downarrow & & & & \downarrow & & \downarrow & & \downarrow & & & & \downarrow \\
z_0 & & \cdots & & z_{t-1} & & z_t & & z_{t+1} & & \cdots & & z_N
\end{array}$$

At the SSH Causal Level (which is part of the topological map), exploration experience is described by an alternating sequence of actions and distinctive states, with each distinctive state associated with a view.

$$\begin{array}{ccccccccccc}
q_0 & a_1 & q_1 & a_2 & q_2 & \cdots & q_{n-1} & a_n & q_n \\
| & & | & & | & & | & & | \\
v_0 & & v_1 & & v_2 & \cdots & v_{n-1} & & v_n
\end{array}$$

In both the basic and hybrid versions of the SSH, distinctive states q correspond to being at a place, facing along a directed path. In the basic SSH, the distinctive states q are grounded by isolated distinctive states $\bar{x}$ where hill-climbing control laws terminate. In the Hybrid SSH, dstates are grounded by a directed local-path extracted from the LPM of a place neighborhood.

At the SSH Topological Level, a particular place p_j can correspond to several distinctive states, say q_{i-1} and q_i and the turn action a_i between them. A travel action a_{i+1} from q_i at p_j to q_{i+1} at a different place p_{j+1} can be used to infer the displacement λ_{j+1}, which is the pose of place p_{j+1} in the frame of reference

[15] There are at most $ml/2$ unique travel actions. There are at most l turns at each of the m places. Thus, in the worst case environment, we have ml turns and $ml/2$ travels, resulting in $3ml/2$ actions in the basic SSH.

[16] Savelli and Kuipers [2004] also point out that for each map m_i in the tree to be expanded, the reduction of the branching factor k_i due to the planarity constraint is proportional to the number of closed loops already present in m_i. In other words, "the more loops [that] have been closed, the more topologically compact the map must be, and therefore the fewer ways there are to close new loops while preserving planarity," which reduces the branching factor further.

of place p_j. This lets us abstract the sequence of distinctive states and actions to an alternating sequence of place p_j and displacements λ_j.

$$p_0 \quad \lambda_1 \quad p_1 \quad \lambda_2 \quad p_2 \quad \cdots \quad p_{m-1} \quad \lambda_m \quad p_m$$

As described in Section 7 and illustrated in Figure 14, in order to define the λ_i, each place neighborhood must have its own frame of reference and we must select a set of distinguished time-points $0 \leq t_0 < t_1 < \cdots \leq t_N = N$ such that adjacent time-points belong to different place neighborhoods, and the pose x_{t_i} at each time-point t_i can be unambiguously localized in its place neighborhood. To fit this into the SSH causal framework, we select distinguished time-points at the termination of each travel action: in the basic SSH, this is after hill-climbing terminates, and in the hybrid SSH, this is after a place is detected. In the Hybrid SSH, the dividing poses are near the incoming gateways in place neighborhoods. The net effect of the turn and travel actions between these dividing points are used to estimate the displacements λ_i between the frames of reference of adjacent place neighborhoods connected by path segments.

7 HSSH Global Metrical Level

The topological map identifies a discrete set of places, each with its own local metrical map within its own frame of reference. The topological map also encodes decisions about how loops are closed and which aliased local neighborhoods represent the same places. The global metrical map is built on the structural skeleton provided by the topological map [Modayil et al., 2004]. The steps in building the global metrical map are: (1) describe the *displacements* $\lambda = \{\lambda_i\}$, each describing the change in pose from one place neighborhood to the next in the frame of reference of the first; (2) describe the *layout* $\chi = \{\chi_p\}$, specifying the poses of places in a global frame of reference; (3) describe the *trajectory* $x = \{x_t\}$ of robot poses within the global frame; and (4) create the *global map* m^* from sensor readings given the trajectory.

7.1 Terminology

The global topology τ, used below, consists of the set $M^P = \{\langle p, m_p, S_p, \psi_p \rangle : p \in P\}$ of places with their local information, the set of distinguished time-points $0 \leq t_0 < t_1 < \cdots < t_n \leq N$ that divide the fine-grained sequence of exploration experience into segments corresponding to travel between adjacent place neighborhoods, and the relation $place(t_i) = p_j$ between them. It is convenient to relabel the variables x, z, and u, defining $x_{i,j} \equiv x_{t_i+j}$. At each distinguished time-point t_i, where $place(t_i) = p_j \in P$ and $place(t_{i+1}) \neq place(t_i)$, the agent is localized in the local metrical map m_{p_j}.

Much of our metrical inference consists of defining an appropriate set of reference frames, and estimating the values of local and non-local metrical quantities. Many of these concepts can be simply understood

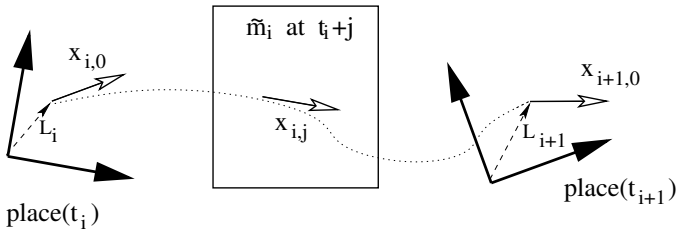

Figure 14: **Defining local frames of reference.** The agent creates the local scrolling map $\tilde{m}_i$ when traveling between places. The agent's poses at the distinguished time-points t_i and t_{i+1} are $L_i = [x_{i,0}]_{place(t_i)}$ and $L_{i+1} = [x_{i+1,0}]_{place(t_{i+1})}$. The displacement between the two place frames of reference is $\lambda_{i+1} = L_i \oplus [x_{i+1,0}]_{\tilde{m}_i} \oplus (\ominus L_{i+1})$.

by examining Figure 14.

$[x]_p$	The coordinates of the pose x in the frame of reference of place p.
O_p	The pose x such that $[x]_p = (0,0,0)$.
$L_i \equiv [x_{t_i}]_{place(t_i)}$	The coordinates of the pose x_{t_i} in the reference frame of $place(t_i)$.
$\tilde{m}_i$	The scrolling map that models the agent's surroundings between distinctive time-points t_i and t_{i+1}. The map's origin is defined as the agent's pose at time t_i. That is, $O_{\tilde{m}_i} = x_{t_i}$.
$\lambda_i \equiv [O_{place(t_i)}]_{place(t_{i-1})}$	The location of $O_{place(t_i)}$ in the reference frame of $place(t_{i-1})$, estimated using the experience from t_{i-1} to t_i.
$\chi_p \equiv [O_p]_{m^*}$	The pose of O_p in the global reference frame of m^*.
m^*	The global metrical map.

7.2 The Theory of the Global Metrical Map

To build a global metrical map m^*, we want to find the maximum-likelihood path the robot traveled, using the topological skeleton in addition to odometry. As discussed in Section 4.1, the joint probability of the pose history x and the global map m^* can be decomposed as

$$P(x, m^*|z, u) = P(m^*|x, z, u) \cdot P(x|z, u)$$

by the chain rule for probabilities. This decomposition is valuable since $P(m^*|x, z, u)$ (map-building given accurate localization) can be computed analytically and incrementally for popular map types, so we can focus our attention on $P(x|z, u)$ (pose estimation).

To include the effect of possible global topologies τ on pose estimation, we marginalize over the space of topologies. If we assume that the correct global topology $\bar{\tau}$ has been identified, only one topological

hypothesis $\tau = \bar{\tau}$ has nonzero probability.

$$\begin{aligned} P(x|z,u) &= \sum_{\tau} P(x|z,u,\tau) \cdot P(\tau|z,u) \\ &= P(x|z,u,\bar{\tau}) \end{aligned}$$

On the other hand, suppose there are multiple topologies τ with significantly non-zero values of $P(\tau|z,u)$. While the weighted sum provides a mathematically correct characterization of the probability distribution $P(x|z,u)$, it can easily lead to a nonsensical metrical map due to the dramatic qualitative impact of topological structure on the metrical map. Thus the summation should be regarded as describing a disjunction over topological maps, with $P(\tau|z,u)$ being the likelihood of each map. This is exactly the tree of possible topological maps we have already constructed. Therefore, even in the case where there are multiple plausible topological maps, we will construct global metrical maps for each one individually.

Given a particular topology $\bar{\tau}$, we can marginalize over the poses of all topological places $\chi = \chi_i$ and their estimated displacements λ.

$$P(x|z,u,\bar{\tau}) = \int\int P(x|\chi,\lambda,z,u,\bar{\tau}) \cdot P(\chi|\lambda,z,u,\bar{\tau}) \cdot P(\lambda|z,u,\bar{\tau})\, d\lambda\, d\chi$$

Because x is conditionally independent of λ given χ, and χ is conditionally independent of z,u given λ, we can simplify this equation.

$$P(x|z,u,\bar{\tau}) = \int P(x|\chi,z,u,\bar{\tau}) \int P(\chi|\lambda,\bar{\tau})\, P(\lambda|z,u,\bar{\tau})\, d\lambda d\chi$$

We divide this equation into simpler components, defining the following functions representing probability distributions over their arguments.[17]

$$\begin{aligned} F(\lambda) &= P(\lambda|z,u,\bar{\tau}) \\ G(\chi) &= \int P(\chi|\lambda,\bar{\tau})\, F(\lambda)\, d\lambda \\ H(x) &= \int P(x|\chi,z,u,\bar{\tau})\, G(\chi)\, d\chi \end{aligned}$$

Thus, we use the topological map $\bar{\tau}$ to factor the localization term $P(x|z,u) = H(x)$ into three separate probability distributions: place-to-place displacements $F(\lambda)$ derived from local metrical maps; the metrical layout $G(\chi)$ of places in the global topological map; and the global metrical layout $H(x)$ of the robot's pose trajectory. Finally, we can combine the pose trajectory with $P(m^*|x,z,u)$ to define the joint distribution $P(x,m^*|z,u)$.

[17] We assume that there is no opportunity for confusion between these probability functions F, G, and H, and the dynamical system functions F, G, and H_i used in Section 3.1.

7.3 Global Mapping Example

Here we detail each step of creating the global map and discuss our current implementation, which runs offline. Figure 15 demonstrates the stages of creating an accurate global metrical map of a large, complex environment using these methods.

7.3.1 Estimating $F(\lambda)$

Given the topology τ, we can compute $F(\lambda)$. Each λ_i corresponds to a single experience of a path segment. Since closing large loops is not a problem when considering a single path segment, traditional SLAM methods may be employed to estimate $F(\lambda)$ by decoupling it into a set of independent probabilities.

$$\begin{aligned} D_i &= z_{i,0}, \ldots, z_{i,n_i}, u_{i,1}, \ldots, u_{i+1,0} \\ F_i(\lambda_i) &= P(\lambda_i | D_{i-1}, L_{i-1}, L_i) \\ F(\lambda) &= \prod_{i=1}^{n} F_i(\lambda_i) \end{aligned}$$

See Figure 14 to understand L. Our current implementation is an incremental maximum-likelihood method [Fox et al., 1999], modeling each $F_i(\lambda_i)$ as a Gaussian.

Using the notation of the compounding operator [Smith et al., 1990], we compute the distribution of λ_i by composing three uncertain vectors: the vector L_{i-1} from $O_{place(t_{i-1})}$ to $x_{i-1,0}$; the vector $[x_{i,0}]_{\tilde{m}_{i-1}}$ from $x_{i-1,0}$ to $x_{i,0}$; and finally the vector $-L_i$ from $x_{i,0}$ to $O_{place(t_i)}$.[18]

$$F_i(\lambda_i) = P(\lambda_i = (L_{i-1} \oplus [x_{i,0}]_{\tilde{m}_{i-1}} \oplus (\ominus L_i)))$$

The essential connection is that the pose $x_{i,0}$ at the end of a path-segment is described in the frame of reference of place p_{i-1} by the expression $L_{i-1} \oplus [x_{i,0}]_{\tilde{m}_{i-1}}$, and simultaneously in the frame of reference of place p_i by L_i.

The problem of estimating $[x_{i,0}]_{\tilde{m}_{i-1}}$ is relatively simple along individual path segments, since loops cannot be involved. The more difficult problem arises from determining $\ominus L_i$ after a loop closure. Here we need to align the map m_{p_i} with a previously stored map m_{p_h} in order to determine $[O_{p_h}]_{p_i}$, which allows us to solve $\ominus L_i$. Matching maps can be expensive and can lead to false positives due to local minima (e.g., two LPMs of a + intersection can be matched four ways). To eliminate this problem, we first align the LPMs based on the locations of corresponding gateways, consistent with m_h, S_h, ψ_h and m_i, S_i, ψ_i, before refining the alignment using the obstacles and free space of the LPMs. (Figure 15(c) omits this gateway alignment

[18] Given two poses a and b, we write $[b]_a$ for the coordinates of b in the frame where a defines the origin [Smith et al., 1990]. Then, $[c]_a = [b]_a \oplus [c]_b$. The inverse operator is $[b]_a = \ominus [a]_b$.

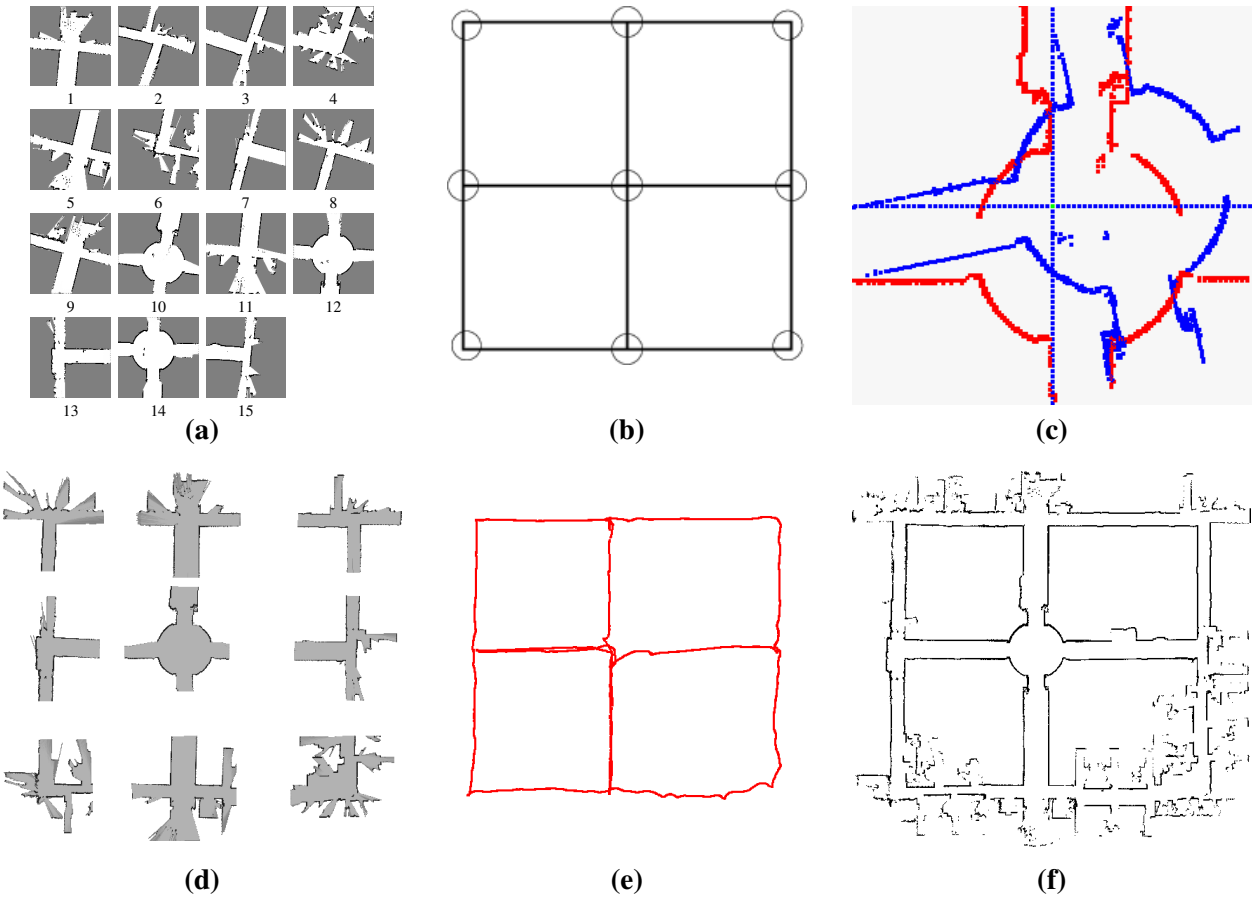

Figure 15: **Global map-building process.** **(a)** The sequence of local place maps m_p experienced. **(b)** The unique topological map consistent with topological and planarity constraints. **(c)** We determine λ_i for loop closures by finding the offset between the current pose and the place origin (defined on the initial place visit). **(d)** The layout χ derived from the topological map and the place-to-place displacements λ. **(e)** The pose trajectory $x(t)$ anchored at points where the robot is localized in place neighborhoods in the layout χ. **(f)** Given the localized pose trajectory $x(t)$ in the global frame of reference, the global metrical map m^* is created accurately and efficiently. Compare with Figure 1.

step in order to better illustrate the process of LPM alignment.)

7.3.2 Estimating $G(\chi)$

The layout $\chi = \{\chi_p\}$ represents the poses of the places in the topological map, with respect to the frame of reference of the global metrical map m^*. $G(\chi)$ is a probability density function over possible layouts χ. Among other things, it reflects the distortion in the place layout due to a loop-closing hypothesis, compared with the observed displacements λ.

Given the topological map, which specifies the data association between observations and places, we can evaluate $G(\chi)$ for an arbitrary distribution of $F(\lambda)$. For a particular value of χ, $P(\chi|\lambda,\bar{\tau})$ will only be non-zero for a single value of λ, namely when each $\lambda_i = (\ominus\chi_{place(t_{i-1})}) \oplus \chi_{place(t_i)}$. Hence, $P(\chi|\lambda,\bar{\tau})$ is a Dirac delta function, which gives us a simple expression for $G(\chi)$.

$$\begin{aligned} G(\chi) &= \int P(\chi|\lambda,\bar{\tau})\, F(\lambda)\, d\lambda \\ &= \prod_{i=1}^{n} F_i((\ominus\chi_{place(t_{i-1})}) \oplus \chi_{place(t_i)}) \end{aligned}$$

When $F(\lambda)$ is represented as a Gaussian, an Extended Kalman Filter (EKF) is a simple way to approximate $G(\chi)$. The idea is to consider place p to be a landmark with pose χ_p. These landmarks are observed one at a time, linked by actions λ_i. This is essentially the classic approach of Smith et al. [1990]. Given Gaussian uncertainty along each action u_i connecting the n robot poses, along with constraints that give Gaussian uncertainty between poses taken from multiple visits to the same place (to associate poses after loop closures), we can solve for $H(x)$ in time $O(n \log n)$ using the sparse matrix methods of Konolige [2004]. However, often we may only want $G(\chi)$, which can be computed in $O(m \log m)$ time for m places, where $m \ll n$.

In our current implementation, we utilize a hill-climbing search to quickly converge to a local maximum of $G(\chi)$ (Figure 15(d)). The Levenberg-Marquardt algorithm for nonlinear optimization [Press et al., 1992] treats the λ_i as "springs" between the poses of the places p_k in χ, and relaxes their configuration to reach a local minimum-energy configuration. Efficient estimations of this non-linear optimization also exist [Olson et al., 2006]. A good initial layout χ for this hill-climbing search can be derived from the displacements λ_i, which represent SLAM-corrected odometry from the scrolling map. We use the term $\hat{\chi}$ to denote the computed estimate of $G(\chi)$.

7.3.3 Estimating $H(x)$

An extended Kalman filter can be used to estimate $H(x)$ using $G(\chi)$ and individual pose covariances from the experienced trajectory. Alternatively, if accurate pose covariances are not available, a simple method

can estimate the maximum-likelihood trajectory through the environment. We calculate the independent trajectory $H_i(x)$ along each path segment, as each place location is fully determined by a global layout χ. In most cases, there will be some discrepancy between the measured distance λ_i along the path segment and the fixed distance between the places in χ. We transform the experienced motion along the path segment to fit the global path segment distance using a simple affine transformation. This process is similar to methods of distributing odometry error after closing a loop in a global metrical map [Thrun et al., 2000a].

For each trajectory between adjacent places p_i and p_{i+1}, we transform the relative, incremental displacements $\Delta(\mathrm{x},\mathrm{y},\theta)$ from the pose estimates in the scrolling LPM $\tilde{m}_i$ into relative displacements $\xi_{i,j}$ in the global frame of reference. This uses a simple affine transformation T_i to anchor the beginning of the LPM experience to the global frame of reference.

$$\begin{aligned} [x_{i,0}]_{m^*} &= \chi_{place_{t_i}} \oplus L_i \\ [x_{i,j}]_{m^*} &\equiv T_i([x_{i,j}]_{\tilde{m}_i}) \\ \xi_{i,j} &\equiv [x_{i,j}]_{m^*} - [x_{i,j-1}]_{m^*} \end{aligned}$$

We compute a final trajectory for x from the set of incremental displacements $\hat{\xi}$ by satisfying the constraint that the travel experience between the places must fit the globally defined distance between the places. This uses another affine transformation T_i' to map the final pose along the path segment (x_{i,n_i}) to the global frame of reference.

$$\begin{aligned} [x_{i+1,0}]_{m^*} &= \chi_{place_{t_{i+1}}} \oplus L_{i+1} \\ [x_{i+1,0}]_{m^*} - [x_{i,0}]_{m^*} &\equiv T_i'([x_{i,n_i}]_{m^*} - [x_{i,0}]_{m^*}) \equiv T_i'(\sum_{j=1}^{n_i} \xi_{i,j}) \\ \hat{\xi}_{i,j} &\equiv T_i'(\xi_{i,j}) \end{aligned}$$

7.3.4 Creating a map m^*

The trajectory above can be used as a starting trajectory for gradient descent methods to align the pose positions with map estimates to converge upon a locally optimal map [Lu and Milios, 1997; Thrun et al., 2000a]. A more principled approach is to run a Rao-Blackwellized particle-filtering algorithm, using the maximum-likelihood trajectory as the mean of a proposal distribution: $P(x,m|z,u) = P(m|x,z,u) \cdot H(x)$. However, we have found that in practice the x values defined by the above scaling method adequately approximate the mode of the posterior [Modayil et al., 2004]; thus the global map can be built by projecting the recorded range measurements from poses in the new global coordinates. The final map produced from the topological skeleton is shown in Figure 15(f). Compare this to Figure 1(d) to see the improved map.

8 Summary

We have presented a hybrid metrical/topological framework that processes information at both small-scale and large-scale abstractions. Our *Hybrid Spatial Semantic Hierarchy* is inspired by human cognitive maps; thus, it represents the environment using human-like concepts, such as places and paths, which support hierarchical navigation, human-robot interaction, and logical reasoning. Specifically, we focused on the problem of map-building—discussing how the HSSH builds metrical representations for local small-scale spaces, finds a topological map representing the qualitative structure of large-scale space, and constructs a metrical representation for large-scale space in a single global frame of reference by building on the skeleton provided by the topological map.

Unlike many robotic implementations that attempt to build a monolithic, Cartesian global metrical map, we propose an alternative approach that handles closing large loops by hypothesizing symbolic place matches. This ensures all possible loop closures are considered, not just ones where the robot, with accumulated odometry error, happens to be near some older portion of the map. The minimal topological map that results from large-scale exploration is sufficient for navigation and necessary for efficient planning, especially to rule out alternative topological structures during exploration.

The thrust of this paper has been to formally describe how concepts of large-scale space can be grounded in the robot's low-level observations. This problem has hindered topological map-building research, as it is an example of the hard AI problem of *symbol grounding* [Harnad, 1990]. Our innovation has been to utilize metrical approaches to model the immediate, local surround of the robot in order to ground *gateways* in small-scale space. Gateways provide the robot with local motion targets that facilitate control along paths. They also provide a *local topology* description of the local surround, useful for detecting and describing places and the paths that emanate from places.

We demonstrated an implementation of the HSSH within an environment with fairly large, nested loop closures. The results support our claims of efficient, online map-building in the presence of multiple loop closures. We demonstrated that a global layout of places is easily achieved given a topological map hypothesis, and a full global metrical map can be accurately achieved by filling in exploration experience along the path segments that connect places in the environment.

9 Future Work

There are obvious avenues of future work at all levels of the Hybrid SSH: creating semantically labeled LPMs using vision, demonstrating a Hybrid SSH interface that improves human-robot navigation tasks, and exploring very large environments to demonstrate claims about scalability. Below we discuss several specific issues that relate directly to the issues in the paper.

9.1 Formal Description and Evaluation of Gateways

We provided an initial algorithm for gateway detection that works in well-structured LPMs with boundaries on both sides of the underlying paths. This was used to make all gateways figures in this article. Additionally, Figure 13 shows a real-world example of an implementation for gateway identification, place detection, and local topology abstraction. We plan to publish a comprehensive article on a new gateway implementation that works for both corridor and coastal navigation paths (Figure 11). We expect the article to include a formal description of the new algorithm, along with another real-world evaluation, and experiments quantifying the robustness of finding gateways and correct local topology with respect to LPM noise, size, and affine transformations.

9.2 Efficient Expansion of the Tree of Maps

Currently, the tree of maps contains every topological map consistent with exploration experience and the topological axioms. This guarantees soundness, which is useful in the case where observations refute the current best map and the next best map must be identified. However, there remain two related problems that need to be addressed in future work. First is the need for a reliable method to identify the best candidate among a set of possible topological maps, given odometry and perceptual information [Ranganathan et al., 2006]. Second, is the need to reduce the tree of maps from a "breadth-first" search to a more focused search that tracks a small number of maps at a time.

In Section 6.3, we identified the "best" map as the simplest one based on a prioritized circumscription policy over the models generated by the non-monotonic theory of topological maps [Remolina and Kuipers, 2004]. This is sufficient for the environment in Figure 15, but Savelli and Kuipers [2004] describe larger environments where extreme symmetry and aliasing cannot so easily be resolved by purely qualitative methods, as the tree of maps grows too large to maintain in real-time.[19] These are not entirely unrealistic examples, since large grid-structured neighborhoods in real cities provide opportunities for vast topological ambiguity [Lynch, 1960].

One obvious improvement that will limit the number of map hypotheses is to perform *active exploration* that occasionally exploits knowledge of asymmetries in the environment to eliminate entire branches from the tree of maps. Such strategies are similar to the localization procedures advocated by proponents of DFA-style maps [Kuipers and Byun, 1991; Dean et al., 1995; Rekleitis et al., 1999]. Dudek et al. [1991] propose an exploration algorithm that finds the correct topological structure in polynomial number of travel actions, but this requires the robot to drop markers and backtrack to determine which loop-closing hypothesis was correct.

[19] Ranganathan and Dellaert [2005] claim that because (in the worst case) the number of aliased places grows with the amount of exploration experience, the number of possible topological maps is given by Bell's number, which grows hyper-exponentially with the number of perceptually aliased places.

Along with exploration strategies, we would like reduce the tree of maps by drawing on perceptual information currently unused in the topological map-building process. We should be able to use observational data, such as the likelihood of the global metrical layout $P(\hat{\chi}|\lambda, \bar{\tau})$, probabilistic local topology matching, or the likelihood of visual observations at places [Cummins and Newman, 2008], to define weights on the tree of maps. These weights should allow us to have a quantitative ordering on the map hypotheses, and should allow best-first expansion of the tree that focuses on a limited number of highly ranked candidates at a time. This should allow the robot to map larger environments including those with large amounts of symmetry and perceptual aliasing.

References

D. Angluin. On the complexity of minimum inference of regular sets. *Information and Control*, 39:337–350, 1978.

P. Beeson. *Creating and Utilizing Symbolic Representations of Spatial Knowledge using Mobile Robots*. PhD thesis, The University of Texas at Austin, 2008.

P. Beeson, N. K. Jong, and B. Kuipers. Towards autonomous topological place detection using the extended Voronoi graph. In *Proceedings of the IEEE International Conference on Robotics and Automation (ICRA)*, pages 4373–4379, Barcelona, Spain, 2005.

P. Beeson, M. MacMahon, J. Modayil, A. Murarka, B. Kuipers, and B. Stankiewicz. Integrating multiple representations of spatial knowledge for mapping, navigation, and communication. In *Proceedings of the Symposium on Interaction Challenges for Intelligent Assistants*, AAAI Spring Symposium Series, pages 1–9, Stanford, CA, 2007. AAAI Technical Report SS-07-04.

J.-L. Blanco, J.-A. Fernández-Madrigal, and J. González. Toward a unified bayesian approach to hybrid metric-topological SLAM. *IEEE Transactions on Robotics*, 24(2):259–270, April 2008.

J. Borenstein and Y. Koren. The Vector Field Histogram—fast obstacle avoidance for mobile robots. *IEEE Transactions on Robotics and Automation*, 7(3):278–288, 1991.

M. Bosse, P. Newman, J. Leonard, M. Soika, W. Feiten, and S. Teller. An Atlas framework for scalable mapping. In *Proceedings of the IEEE International Conference on Robotics and Automation (ICRA)*, pages 1899–1906, Taipei, Taiwan, 2003.

P. Buschka. *An Investigation of Hybrid Maps for Mobile Robots*. PhD thesis, Örebro University, 2005.

C.-H. Choi, J.-B. Song, W. Chung, and M. Kim. Topological map building based on thinning and its application to localization. In *Proceedings of the IEEE/RSJ Conference on Intelligent Robots and Systems (IROS)*, pages 552–557, Lausanne, Switzerland, 2002.

H. Choset and K. Nagatani. Topological simultaneous localization and mapping (SLAM): toward exact localization without explicit localization. *IEEE Transactions on Robotics and Automation*, 17(2):125–137, April 2001.

E. Chown, S. Kaplan, and D. Kortenkamp. Prototypes, location, and associative networks (PLAN): Towards a unified theory of cognitive mapping. *Cognitive Science*, 19(1):1–51, 1995.

M. Cummins and P. Newman. FAB-MAP: Probabilistic localization and mapping in the space of appearance. *International Journal of Robotics Research*, 27(6):647–665, 2008.

M. Cummins and P. Newman. Probabilistic appearance based navigation and loop closing. In *Proceedings of the IEEE International Conference on Robotics and Automation (ICRA)*, pages 2042–2048, Rome, Italy, 2007.

T. Dean, D. Angluin, K. Basye, S. Engelson, L. Kaelbling, E. Kokkevis, and O. Maron. Inferring finite automata with stochastic output functions and an application to map learning. *Machine Learning*, 18(1): 81–108, 1995.

T. Duckett and U. Nehmzow. Exploration of unknown environments using a compass, topological map and neural network. In *Proceedings of the IEEE International Symposium on Computational Intelligence in Robotics and Automation (CIRA)*, pages 312–317, Monterey, California, 1999.

T. Duckett and A. Saffiotti. Building globally consistent gridmaps from topologies. In *Proceedings of the International IFAC Symposium on Robot Control (SYROCO)*, pages 357–361, Vienna, Austria, 2000.

G. Dudek, M. Jenkin, E. Milios, and D. Wilkes. Robotic exploration as graph construction. *IEEE Transactions on Robotics and Automation*, 7(6):859–865, 1991.

G. Dudek, P. Freedman, and S. Hadjres. Using local information in a non-local way for mapping graph-like worlds. In *Proceedings of the International Joint Conference on Artificial Intelligence (IJCAI)*, pages 1639–1647, Chambéry, France, 1993.

A. Elfes. *Occupancy Grids: A Probabilistic Framework for Robot Perception and Navigation*. PhD thesis, Carnegie Mellon University, 1989.

A. Eliazar and R. Parr. DP-SLAM: Fast, robust simultaneous localization and mapping without predetermined landmarks. In *Proceedings of the International Joint Conference on Artificial Intelligence (IJCAI)*, pages 1135–1142, Acapulco, Mexico, 2003.

S. Fortune. Voronoi diagrams and Delaunay triangulations. In D.-Z. Du and F. Hwang, editors, *Computing in Euclidean Geometry*, volume 1 of *Lecture Notes Series on Computing*, pages 193–234. World Scientific, 1992.

D. Fox, W. Burgard, and S. Thrun. The dynamic window approach to collision avoidance. *IEEE Robotics & Automation Magazine*, 4(1), March 1997.

D. Fox, W. Burgard, and S. Thrun. Markov localization for mobile robots in dynamic environments. *Journal of Artificial Intelligence Research*, 11:391–427, 1999.

T. Gladwin. *East is a Big Bird: Navigation and Logic on Puluwat Atoll*. Harvard University Press, Cambridge, Massachusetts, 1970.

E. M. Gold. Complexity of automaton identification from given sets. *Information and Control*, 37:302–320, 1978.

D. Hähnel, W. Burgard, D. Fox, and S. Thrun. An efficient FastSLAM algorithm for generating maps of large-scale cyclic environments from raw laser range measurements. In *Proceedings of the IEEE/RSJ Conference on Intelligent Robots and Systems (IROS)*, pages 206–211, Las Vegas, Nevada, 2003a.

D. Hähnel, S. Thrun, B. Wegbreit, and W. Burgard. Towards lazy data association in SLAM. In *Proceedings of the International Symposium on Robotics Research (ISRR)*, pages 83–105, Sienna, Italy, 2003b.

S. Harnad. The symbol grounding problem. *Physica D*, 42:335–346, 1990.

B.-Y. Ko, J.-B. Song, and S. Lee. Real-time building of a thinning-based topological map with metric features. In *Proceedings of the IEEE/RSJ Conference on Intelligent Robots and Systems (IROS)*, pages 797–802, Sendai, Japan, 2004.

S. Koenig and R. G. Simmons. Unsupervised learning of probabilistic models for robot navigation. In *Proceedings of the IEEE International Conference on Robotics and Automation (ICRA)*, pages 2301–2308, Minneapolis, Minnesota, 1996.

K. Konolige. Large-scale map-making. In *Proceedings of the National Conference on Artificial Intelligence (AAAI)*, pages 457–463, San Jose, California, 2004.

K. Konolige. A gradient method for realtime robot control. In *Proceedings of the IEEE/RSJ Conference on Intelligent Robots and Systems (IROS)*, pages 639–646, Takamatsu, Japan, 2000.

D. Kortenkamp and T. Weymouth. Topological mapping for mobile robots using a combination of sonar and vision sensing. In *Proceedings of the National Conference on Artificial Intelligence (AAAI)*, pages 979–984, Seattle, Washington, 1994.

J. J. Kuffner and S. M. LaValle. RRT-Connect: An efficient approach to single-query path planning. In *Proceedings of the IEEE International Conference on Robotics and Automation (ICRA)*, pages 995–1001, San Francisco, California, 2000.

B. Kuipers. The Spatial Semantic Hierarchy. *Artificial Intelligence*, 119:191–233, 2000.

B. Kuipers. An intellectual history of the Spatial Semantic Hierarchy. In M. E. Jefferies and W.-K. Yeap, editors, *Robotics and Cognitive Approaches to Spatial Mapping*, volume 38 of *Springer Tracts in Advanced Robotics*, pages 243–264. Springer, Berlin, Germany, 2008.

B. Kuipers and P. Beeson. Bootstrap learning for place recognition. In *Proceedings of the National Conference on Artificial Intelligence (AAAI)*, pages 174–180, Edmonton, Canada, 2002.

B. Kuipers, J. Modayil, P. Beeson, M. MacMahon, and F. Savelli. Local metrical and global topological maps in the Hybrid Spatial Semantic Hierarchy. In *Proceedings of the IEEE International Conference on Robotics and Automation (ICRA)*, pages 4845–4851, New Orleans, Louisiana, 2004.

B. J. Kuipers. Modeling spatial knowledge. *Cognitive Science*, 2:129–153, 1978.

B. J. Kuipers and Y.-T. Byun. A robot exploration and mapping strategy based on a semantic hierarchy of spatial representations. *Journal of Robotics and Autonomous Systems*, 8:47–63, 1991.

A. Lankenau, T. Röfer, and B. Krieg-Brückner. Self-localization in large-scale environments for the bremen autonomous wheelchair. In *Spatial Cognition III*, volume 2685 of *Lecture Notes in Artificial Intelligence*, pages 34–61. Springer-Verlag, Berlin, Germany, 2002.

W.-Y. Lee. *Spatial Semantic Hierarchy for a Physical Mobile Robot*. PhD thesis, The University of Texas at Austin, 1996.

J. Leonard and P. Newman. Consistent, convergent, and constant-time SLAM. In *Proceedings of the International Joint Conference on Artificial Intelligence (IJCAI)*, pages 1143–1150, Acapulco, Mexico, 2003.

V. Lifschitz. Nested abnormality theories. *Artificial Intelligence*, 74:351–365, 1995.

F. Lu and E. Milios. Globally consistent range scan alignment for environment mapping. *Autonomous Robots*, 4:333–349, 1997.

K. Lynch. *The Image of the City*. MIT Press, Cambridge, Massachusetts, 1960.

M. MacMahon, B. Stankiewicz, and B. J. Kuipers. Walk the talk: Connecting language, knowledge, action in route instructions. In *Proceedings of the National Conference on Artificial Intelligence (AAAI)*, pages 1475–1482, Boston, Massachusetts, 2006.

M. J. Mataric. Integration of representation into goal-driven behavior-based robots. *IEEE Transactions on Robotics and Automation*, 8(3):304–312, 1992.

J. Modayil, P. Beeson, and B. Kuipers. Using the topological skeleton for scalable, global, metrical map-building. In *Proceedings of the IEEE/RSJ Conference on Intelligent Robots and Systems (IROS)*, pages 1530–1536, Sendai, Japan, 2004.

M. Montemerlo, S. Thrun, D. Koller, and B. Wegbreit. FastSLAM: a factored solution to the simultaneous localization and mapping problem. In *Proceedings of the National Conference on Artificial Intelligence (AAAI)*, pages 593–598, Edmonton, Canada, 2002.

M. Montemerlo, S. Thrun, D. Koller, and B. Wegbreit. FastSLAM 2.0: an improved particle filtering algorithm for simultaneous localization and mapping that provably converges. In *Proceedings of the International Joint Conference on Artificial Intelligence (IJCAI)*, pages 1151–1156, Acapulco, Mexico, 2003.

H. P. Moravec. Sensor fusion in certainty grids for mobile robots. *AI Magazine*, pages 61–74, Summer 1988.

A. C. Morris, D. Silver, D. Ferguson, and S. Thayer. Towards topological exploration of abandoned mines. In *Proceedings of the IEEE International Conference on Robotics and Automation (ICRA)*, pages 2117–2123, Barcelona, Spain, 2005.

A. Murarka, J. Modayil, and B. Kuipers. Building local safety maps for a wheelchair robot using vision and lasers. In *Proceedings of the Canadian Conference on Computer and Robot Vision (CRV)*, page 25, Quebec City, Canada, 2006.

E. Olson, J. Leonard, and S. Teller. Fast iterative optimization of pose graphs with poor initial estimates. In *Proceedings of the IEEE International Conference on Robotics and Automation (ICRA)*, pages 2262–2269, Orlando, Florida, 2006.

M. A. Paskin. Thin junction tree filters for simultaneous localization and mapping. In *Proceedings of the International Joint Conference on Artificial Intelligence (IJCAI)*, pages 1157–1166, Acapulco, Mexico, 2003.

W. H. Press, S. A. Teukolsky, W. T. Vitterling, and B. P. Flannery. *Numerical Recipes in C: The Art of Scientific Computing*. Cambridge University Press, London, second edition, 1992.

A. Ranganathan and F. Dellaert. Data driven MCMC for appearance-based topological mapping. In *Proceedings of Robotics: Science and Systems (RSS)*, pages 209–216, Cambridge, Massachusetts, 2005.

A. Ranganathan, E. Menegatti, and F. Dellaert. Bayesian inference in the space of topological maps. *IEEE Transactions on Robotics*, 22(1):92–107, February 2006.

I. M. Rekleitis, V. Dujmovic, and G. Dudek. Efficient topological exploration. In *Proceedings of the IEEE International Conference on Robotics and Automation (ICRA)*, pages 676–681, Detroit, Michigan, 1999.

E. Remolina and B. Kuipers. Towards a general theory of topological maps. *Artificial Intelligence*, 152: 47–104, 2004.

R. L. Rivest and R. E. Schapire. Inference of finite automata using homing sequences. In *Proceedings of the ACM Symposium on Theory of Computing (STOC)*, pages 411–420, Seattle, Washington, 1989.

F. Savelli and B. Kuipers. Loop-closing and planarity in topological map-building. In *Proceedings of the IEEE/RSJ Conference on Intelligent Robots and Systems (IROS)*, pages 1511–1517, Sendai, Japan, 2004.

R. E. Schapire. The design and analysis of efficient learning algorithms. Technical report, MIT Laboratory for Computer Science, 1991. MIT/LCS/TR-493.

D. Schröter. *Region & Gateway Mapping: Acquiring Structured and Object-Oriented Representations of Indoor Environments.* PhD thesis, Technical University of Munich, 2006.

D. Schröter, T. Weber, M. Beetz, and B. Radig. Detection and classification of gateways for the acquisition of structured robot maps. In *Proceedings of the Symposium of the German Association for Pattern Recognition (DAGM)*, pages 553–561, Tübingen, Germany, 2004.

H. Shatkay and L. P. Kaelbling. Learning topological maps with weak local odometric information. In *Proceedings of the International Joint Conference on Artificial Intelligence (IJCAI)*, pages 920–929, Nagoya, Japan, 1997.

A. W. Siegel and S. H. White. The development of spatial representations of large-scale environments. In H. W. Reese, editor, *Advances in Child Development and Behavior*, volume 10, pages 9–55. Academic Press, New York, 1975.

D. Silver, D. Ferguson, A. C. Morris, and S. Thayer. Feature extraction for topological mine maps. In *Proceedings of the IEEE/RSJ Conference on Intelligent Robots and Systems (IROS)*, pages 773–779, Sendai, Japan, 2004.

R. Smith, M. Self, and P. Cheeseman. Estimating uncertain spatial relationships in robotics. In I. J. Cox and G. T. Wilfong, editors, *Autonomous Robot Vehicles*, pages 167–193. Springer Verlag, New York, 1990.

S. Thrun and A. Bücken. Integrating grid-based and topological maps for mobile robot navigation. In *Proceedings of the National Conference on Artificial Intelligence (AAAI)*, pages 944–950, Portland, Oregon, 1996.

S. Thrun, S. Gutmann, D. Fox, W. Burgard, and B. J. Kuipers. Integrating topological and metric maps for mobile robot navigation: A statistical approach. In *Proceedings of the National Conference on Artificial Intelligence (AAAI)*, pages 989–995, Madison, Wisconsin, 1998.

S. Thrun, W. Burgard, and D. Fox. A real-time algorithm for mobile robot mapping with applications to multi-robot and 3d mapping. In *Proceedings of the IEEE International Conference on Robotics and Automation (ICRA)*, pages 321–328, San Francisico, California, 2000a.

S. Thrun, D. Fox, and W. Burgard. Monte Carlo localization with mixture proposal distribution. In *Proceedings of the National Conference on Artificial Intelligence (AAAI)*, pages 859–865, Austin, Texas, 2000b.

S. Thrun, W. Burgard, and D. Fox. *Probabilistic Robotics*. MIT Press, Cambridge, Massachusetts, 2005.

N. Tomatis, I. Nourbakhsh, and R. Siegwart. Hybrid simultaneous localization and map building: Closing the loop with multi-hypotheses tracking. In *Proceedings of the IEEE International Conference on Robotics and Automation (ICRA)*, pages 2749–2754, Washington, DC, 2002.

J. O. Wallgrün. Autonomous construction of hierarchical voronoi-based route graph representations. In *Spatial Cognition IV. Reasoning, Action, Interaction*, volume 3343 of *Lecture Notes in Artificial Intelligence*, pages 413–433. Springer-Verlag, Berlin, Germany, 2005.

M. Yannakakis and D. Lee. Testing finite state machines. In *Proceedings of the ACM Symposium on Theory of Computing (STOC)*, pages 476–485, New Orleans, Louisiana, 1991.

W.-K. Yeap. Towards a computational theory of cognitive maps. *Artificial Intelligence*, 34:297–360, 1988.

W.-K. Yeap and M. E. Jefferies. Computing a representation of the local environment. *Artificial Intelligence*, 107(2):265–301, 1999.

T. Y. Zhang and C. Y. Suen. A fast parallel algorithm for thinning digital patterns. *Communications of the ACM*, 27(3):236–239, March 1984.

U. R. Zimmer. Embedding local metrical map patches in a globally consistent topological map. In *Proceedings of the International Symposium on Underwater Technology (UT)*, pages 301–305, Tokyo, Japan, 2000.